Environmental
Science
Nano

ROYAL SOCIETY
OF CHEMISTRY

PAPER

View Article Online
View Journal | View Issue

Cite this: *Environ. Sci.: Nano*, 2026, **13**, 478

Sublethal effects of photoactive engineered nanomaterials on filamentous bacteriophage infection and *E. coli* gene expression in freshwater

Shushan Wu, Stefanie Huttelmaier, Jack Sumner,
Erica Hartmann and Kimberly Gray*

Received 1st July 2025,
Accepted 3rd December 2025

DOI: 10.1039/d5en00598a

rsc.li/es-nano

Wide application and release of engineered nanomaterials (ENMs) into the environment require an understanding of their potential ecological impacts, particularly under real environmental conditions. Previously we reported that low doses of photoexcited ENMs exert significant sublethal stress on bacterial outer membranes in a freshwater medium, potentially increasing bacterial susceptibility to viral infection and promoting microbial evolution and diversity. However, little is known about how ENMs may affect bacteriophage infection under environmental conditions. Therefore, this study investigates the effects of commonly used photoactive ENMs – n-TiO_2, n-Ag, and their mixtures – on the infection of a filamentous coliphage, bacteriophage f1, at environmentally relevant concentrations under freshwater conditions. We also interrogate cellular surface properties and the expression of key genes associated with phage–cell interactions in response to ENM exposure. Under light, n-TiO_2 or n-Ag increases bacteriophage infection, consistent with trends showing increased outer membrane permeability (OMP), F-pili-related gene expression, and pili density. Exposure to n-TiO_2 + n-Ag mixtures under light, however, suppresses the effects of the individual ENMs on bacteriophage infection, despite high OMP, amplified up-regulation in F-pili and membrane protein expression, and augmented pili density. We propose that greater oxidative stress on the cell membrane induced by the photoexcited ENM mixtures in comparison to individual ENM exposure, as previously detailed, damages membrane proteins (*e.g.*, TolA) vital to bacteriophage entry and dominates other mechanisms. Overall, our results provide mechanistic insight into the complex interactions among bacteria, bacteriophage, and ENMs, under environmentally relevant conditions, and further detail their potential ecological risks.

Environmental significance

Mass production and release of engineered nanomaterials (ENMs) raise ecotoxicity concerns. Previously, we found that photoactive ENMs exert sublethal bacterial stress under environmental conditions which may alter the patterns of bacteriophage infection and consequently, impact microbial diversity and evolution. Yet, ENMs' influence on bacteriophage infection under environmental conditions remains largely unexplored. In this study, filamentous phage infection was promoted by exposure to individual ENMs under light in freshwater but suppressed by n-TiO_2 + n-Ag mixtures. Although both exposure conditions caused increased outer membrane permeability, up-regulated bacterial genes, and augmented pili density, their differential effects on phage infection were explained by damage to the periplasmic protein, associated with higher ROS yields and greater outer membrane damage by the ENM mixtures.

1 Introduction

Rapid commercialization of nanotechnology has led to massive growth in the production and application of engineered nanomaterials (ENMs) in industrial, agricultural, pharmaceutical, and personal care sectors over the last two decades.[1–3] As a result, the release and accumulation of ENMs into the environment due to the lack of regulation or effective treatment strategies raise serious concerns about the ecological impacts of ENMs.[4,5] The toxicity of ENMs on humans,[6] animals,[7] and microorganisms in different environments (*e.g.*, terrestrial, freshwater, and marine)[8–10] has been well studied, and the effects of key environmental conditions, such as light, ionic composition of the media,

Department of Civil and Environmental Engineering, Northwestern University, Tech A236, 2145 Sheridan Road, Evanston, IL, 60208, USA.
E-mail: shushan.wu@northwestern.edu, stefaniehuttelmaier2024@u.northwestern.edu, jacksumner2026@u.northwestern.edu, erica.hartmann@northwestern.edu, k-gray@northwestern.edu

and natural organic matter, on the properties and behaviors of ENMs have also been addressed.[11] However, ENMs effects on viruses in the environment remain largely unexplored.

Bacteriophages, or phages, are viruses that invade bacterial cells and inject their genomes into the bacterial hosts. They are highly diverse and among the most abundant biological entities in the environment with numbers more than 10 times of bacterial counts, ranging from 10^4 to 10^8 viral particles per milliliter in natural waters.[12–14] Their ubiquity and ability to alter bacterial genetic material make phages a significant driving force in the diversity, population dynamics, and evolution of bacteria in ecosystems. Thus, to better interpret and predict the ecological impact of ENMs, it is crucial to evaluate the effects of ENMs on phages and phage infection, especially in natural or engineered environmental settings. Yet, studies reporting relevant findings are scarce.

Limited available data show that ENMs, depending on their physiochemical properties (*e.g.*, type, solubility, zeta potential, and concentration), can affect phage infection by binding to the phage protein capsid, altering the protein structure, interfering with phage–host interactions, and disrupting the host cell's normal functions which indirectly influences the phage life cycle (Table S1). Most studies focus on the inactivation of phage by ENM exposure due to the antibacterial properties of ENMs, including nZVI[15–19] and n-Ag.[20] n-Ag is used in the greatest number of products because of its low cost and strong antibacterial properties.[21] Gilcrease *et al.*[20] reported an inhibitory effect of uncoated n-Ag (10 mg L^{-1}, suspended in citrate) on phage infection, resulting from n-Ag binding to the phage capsid protein and disruption of phage–host interactions, while PVP-coated n-Ag increased phage infection greatly as PVP coating lowered negativity in zeta potential and reduced biological activities of n-Ag. Similarly, You *et al.*[22] exposed phage MS2 and phage/*E. coli* suspension to 1–5 mg L^{-1} PVA-capped n-Ag (~21 nm) and observed an increase in the phage infection when phage and bacteria were simultaneously exposed to n-Ag.

Zhang *et al.*[23] observed increases in phage transduction efficiency of planktonic *E. coli* bacteria when exposed to 0.01–10 mg L^{-1} of uncoated n-Ag with the maximum effect of a 3-fold increase induced by 0.1 mg L^{-1} n-Ag. Transduction, mediated by phage, is a horizontal gene transfer pathway that allows genetic material to pass from one bacterium to another *via* phage infection. It plays a vital, yet largely unexplored, role in the spread of antibiotic resistance genes (ARGs) in natural and anthropogenic environments.[24–28] Zhang *et al.*[23] suggested a mechanism promoted by n-Ag as well as released Ag^+ enhancing intracellular oxidative stress and increasing outer membrane permeability (OMP). They proposed that the binding of n-Ag by the phage facilitated the transport of n-Ag to the bacterial cell surface, which also contributed to increased phage transduction.

Other metal-based ENMs, such as n-TiO_2,[29,30] n-CuO,[31] and n-ZnO,[22] are reported to increase phage infection because of electrostatically enhanced phage–host interaction at the cell surface. Exposure to ENMs induces bacterial stress, altering cellular structures and interfering with gene expression,[11] which contributes to the infectious entry of phage to the host cell. Previous work showed that n-TiO_2 and n-CuO facilitated phage infection by up-regulating host gene expression related to phage receptors and energy production[29–31] and damaging cell membranes.[29,30,32] Stachurska *et al.*[33] revealed the decisive role of NPs' zeta potential in the binding between NPs and T4-like phage. They proposed that NPs with highly negative zeta potential (<−35 mV) tend to bind to the tail of the phage, which prohibits the attachment of phage to the host cell and consequently, decreases phage infection. In other cases, NPs may work in synergy with phage to facilitate the phage entry to host cells. Specifically, NPs with zeta potential >35 mV bind to the head of the phage, and NPs at zeta potential between −35 mV and 35 mV tend to exhibit non-specific binding. Unstable ENMs, like n-ZnO or n-Ag, release metal cations, which reduce electrostatic barriers between bacteria and phages and promote phage infection.[22]

In real environments, phage infection and propagation are greatly influenced by surrounding environmental conditions, such as light, pH, ionic composition, and organic and inorganic substances.[34,35] Since these factors modify ENM interactions and toxicities toward microbes and bacteria in the environment, they may also exert complex effects between ENMs and phages.[11] For example, photoactive ENMs, like n-TiO_2, exhibit higher toxicity under light irradiation due to ROS generation which can also contribute to phage inactivation.[36–39] Kim *et al.*[40] reported enhanced bacteria and MS2 phage inactivation by Ag^+ in the presence of UV-A and visible light. The enhanced inactivation results from the photoreduction of the Ag–cysteine complex and the formation of monosulfide radicals and Ag^0, leading to protein damages on the phage and in cells.[40] Similar phenomena may occur with the release of Ag^+ from the oxidative dissolution of n-Ag.

In contrast, Xiao *et al.*[30] revealed a synergistic effect of photoactivated n-TiO_2 on increasing phage transduction of ARGs. They found that exposure to either n-TiO_2 or UV irradiation alone promoted phage transduction, and exposure to n-TiO_2 (0.5 mM) under UV irradiation (365 nm, 150 μW cm^{-2}) had a synergistic effect on increased phage transduction. This may result from extracellular ROS generated by n-TiO_2 under certain light intensity (<150 μW cm^{-2}) and/or the intracellular ROS triggered by photoactivated n-TiO_2. More specifically, extracellular ROS damaged cell membrane and intracellular ROS induced F-pilus synthesis, contributing to phage entry. However, excessive irradiation may lead to cell death and phage inactivation.[30] These findings revealed, albeit incompletely, the unpredictable impacts of ENMs on phages and phage infection under complex environmental conditions.

In this study, we investigate how two common photoactive ENMs, n-TiO_2 and n-Ag, and their mixtures affect phage infection and the gene expression of *E. coli* in a freshwater environment. Previously we found that in freshwater, photoactive ENMs, like n-TiO_2 and n-Ag, at environmentally relevant concentrations (in μg L^{-1} range) exerted substantial bacterial stress by increasing OMP under simulated sunlight, whereas minimal effects were shown in dark under the same conditions.[41] The effects were more prominent in a freshwater medium than in a synthetic buffer due to different ionic strength and composition, and synergistic effects were observed when exposed to mixtures of n-TiO_2 and n-Ag.[41,42] Such sublethal bacterial stress exerted by ENMs and their mixtures may leave cells more vulnerable to the invasion of surrounding substances, such as toxins and viruses, which may further alter the structure and function of the ecosystem. Therefore, we hypothesize that n-TiO_2 and n-Ag, alone and mixed, at sublethal doses increase phage infection of *E. coli* under light irradiation, due to outer membrane damage, primarily increased permeability or altered cell surface charge, and the associated up-regulation of genes targeting surface structures (*e.g.*, F-pili) and proteins (*e.g.*, TolA) critical to phage entry into the cell.

To test the hypothesis, we expose *E. coli* to the two ENMs, n-TiO_2 and n-Ag, individually and in mixtures, under light and dark in freshwater, and then infect the bacteria with phage f1, a model phage in the F-specific filamentous phage (Ff) family. Unlike most viruses that kill host cells after infection, filamentous phages typically go through a chronic lifecycle that leads to the release of virions without cell lysis and exerts little stress on the bacterial host.[43,44] The Ff phage group specifically infects the bacteria strain *E. coli* K12, and the infection process involves an intricate sequence of events illustrated in Fig. 1. Briefly, the receptor at the tip of the phage first binds with an F-pilus (Fig. 1a), inducing F-pilus retraction to pull the phage into a pore-like structure (a part of the Type IV secretion system that assembles and produces F-pili) and enter the periplasm (Fig. 1b). The tip of the phage then binds with the C-terminal domain, TolAIII, of the TolA protein that is anchored to the inner membrane and extends across the periplasm. The TolA protein brings the phage to the inner membrane where the phage injects its genetic material into the host cell. Filamentous phage may bypass the F-pilus to enter the cell surface, presumably when the outer membrane is damaged (Fig. 1c). The outer membrane protein, OmpF, may also assist the penetration of phage through the cell outer membrane.[45] Once the phage enters the periplasm and binds with the TolA protein, the Tol–Pal protein system brings the outer membrane and inner membrane close together and positions the phage tip to dock on the inner membrane for DNA injection.[43,46]

Given these possible mechanisms of filamentous phage–bacteria interactions, the goal of our research is to detail the acute effects of ENMs on the sequence of events involved in phage f1 infection of *E. coli* in the presence and absence of light, and to explain, then, how phage infection is related to changes at the bacterial cell surface and patterns of gene expression as a function of sublethal ENM exposure over short time intervals.

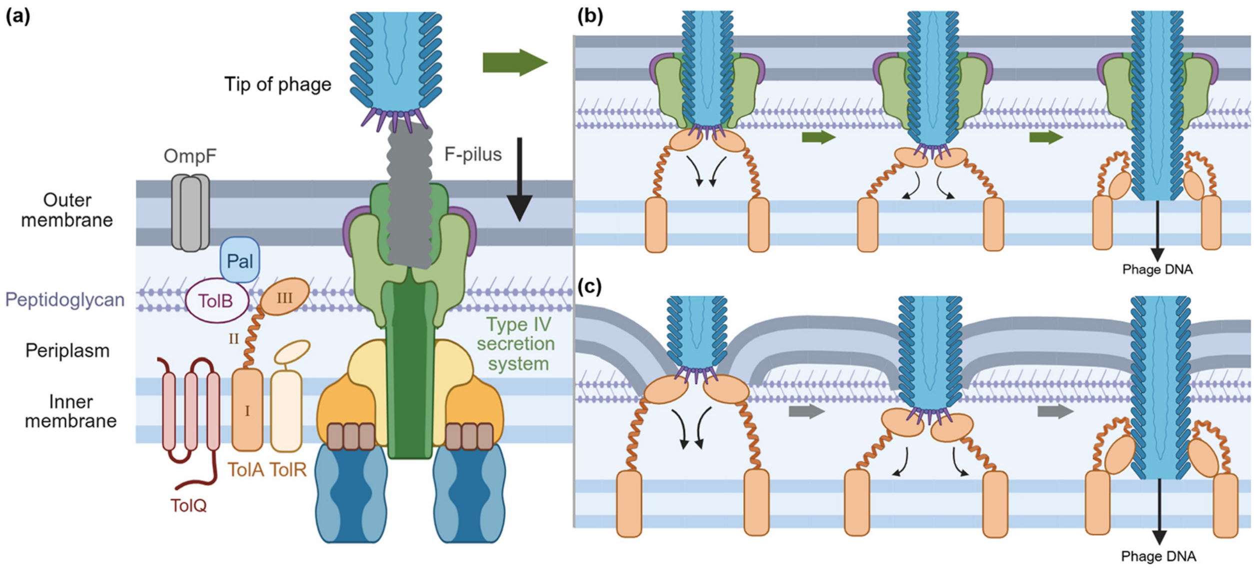

Fig. 1 Process of filamentous phage (Ff group) entering the host cell (*E. coli*) (adapted from Karlsson *et al.*[45] and Hay *et al.*[43]). (a) Phage (tip) first binds to the F-pilus (tip) and activates the retraction of F-pilus. It is unclear how phage penetrates the outer membrane and the cell wall. (b) One popular theory is that upon the retraction of F-pilus, phage is guided into a pore-like structure (a part of the type IV secretion system that assembles the F-pilus), allowing phage to enter the periplasm. Then the protein domain at the tip of the phage binds to the TolA protein, an inner-membrane-anchored protein that extends across the periplasm. The TolA protein positions the phage to dock on the inner membrane, where the phage injects its DNA into the host cell (Riechmann *et al.*[47]). (c) Phage can also bypass the F-pilus and enter the cell, possibly from damaged outer membrane. The Tol–Pal protein system (mainly TolQ-R-A-B and Pal) and the outer membrane porin OmpF assist phage entry by connecting outer and inner membranes, likely associated with the inner to outer membrane adhesion zone (Guihard *et al.*[46]). TolA, after binding to the phage, contracts itself, brings the outer and inner membranes closer, and helps the phage dock on the inner membrane.

2 Materials and methods

2.1 Nanoparticles preparation and environmental medium

Powdered TiO_2 P25 NPs (n-TiO_2 P25, nominal particle size of 22 nm, cat. 384292500) and citrate-stabilized Ag NPs (n-Ag) suspension (10 nm; 1 mg mL^{-1}; 1 mL, aqueous 2 mM sodium citrate; cat. 50-105-6957) were purchased from Thermo Fisher Scientific. n-TiO_2 P25 was suspended in Milli-Q water, sonicated for at least 30 min in an ultrasonic bath (Health-Sonics, 110 W, 42 kHz) to disrupt aggregation, and diluted to make stock solutions with a series of concentrations. n-Ag was diluted with oxygen free Milli-Q water in an anaerobic chamber (MBRAUN UNIlab) to make stock solutions. The characterization of the two NPs, including the hydrodynamic diameters, X-ray diffractogram of n-TiO_2, UV-vis spectra of n-Ag, and TEM micrographs and EDS analysis of the two NPs, are presented in the SI (Fig. S1 and Table S2).

Lake Michigan Water (LMW), collected from the Evanston Drinking Water Treatment Plant, was used in this study as the freshwater medium. The preparation and chemical properties of LMW were reported previously.[41] Briefly, after collecting from the water facility, LMW was stored at 4 °C and filtered through a 0.2 μm PES membrane (Whatman) to remove bacteria and large particles. The pH of LMW is approximately 8.3 and the ionic strength is 3.5 mM.

2.2 Host bacteria culture and phage propagation

E. coli K12 (ATCC 25404) was cultured in Luria-Bertani (LB) broth (with Animal-Free Soytone, L8950, Teknova) at 37 °C overnight and harvested once they reached mid-exponential phase (~18 hours). The cells were then washed with LMW and resuspended in the same media to reach an OD_{600} of 0.4 (± 0.02), which corresponded to the cell concentration of approximately 3×10^8 CFU mL^{-1} as measured by direct plate count.

Bacteriophage f1 (ATCC 15766-B2) was propagated with host *E. coli* K12 in tryptone broth (1% with 0.05 M $CaCl_2$) following the ATCC protocol.[48] Briefly, overnight *E. coli* K12 culture (18 hours old, OD_{600} = 0.4) was prepared and the phage stock was made by adding 0.5 mL broth to the freeze-dried phage vial. To prepare concentrated phage lysate, 100 μL phage stock was added to 5 mL *E. coli* K12 culture and incubated by shaking at 160 rpm in 37 °C overnight for 24 hours. Then, the mixture was centrifuged at 4000*g* for 10 minutes and filtered through a 0.2 μm PES filter. The filtrate was stored at 4 °C for short term (3 months) and −80 °C in glycerol for long term.

2.3 ENM exposure and phage infection measurements

To prevent the inactivation of phage by light irradiation or ENMs,[20,36,49,50] we first exposed *E. coli* to ENMs under light and then added phage lysate and incubated under dark conditions. In this way, we also avoided the effects of light-activated ENMs on phages by minimizing the time of direct ENM contact or exposure as those effects are not the focus of this study. *E. coli* K12 suspension in LMW was prepared as described above with OD_{600} of 0.4 (± 0.02). 0.2 mL ENM stock solution (n-TiO_2 and n-Ag alone or in mixtures) was added to 1.8 mL *E. coli* K12 suspension in a 12-well plate and the final ENMs concentrations are listed in Table 1. Two plates were prepared with one wrapped with clear polyvinyl-chloride film (Fisherbrand™, cat. 01810) that is highly transparent (>90% light transmittance)[51] and exposed to simulated sunlight (SSI) using the Newport 1000 W xenon arc lamp (model #6271 Ozone Free, Newport Corporation, Irvine, CA, USA) and the other covered with aluminum foil to create dark conditions. Both plates were placed on the microplate shaker, rotating at 200 rpm for two hours. Then, 90 μL phage lysate (diluted to 3×10^9 PFU mL^{-1}) was added to each well (cell-to-phage volume ratio of 20 : 1) and mixed in the dark at room temperature for 1 hour. The phage infection was measured by plaque yield using the double-layer-agar method.[52]

The top layer (0.5% agar) and bottom layer (1.5% agar) agar were prepared with tryptone broth (1% with 0.05 M $CaCl_2$). 200 μL of phage/ENMs/bacteria mixture was added to 8 mL of warm top layer agar and mixed before pouring on the plate with the bottom layer agar. After cooling down, the plate was placed upside down and incubated overnight at 37 °C. Plaque counts with 30 to 300 clear plaques were recorded. All experiments were repeated at least three times for accuracy and reproducibility. To better show the sublethal effects, we focus on the results of 0–100 μg L^{-1} n-Ag (Fig. 2). The results of 0–500 μg L^{-1} n-Ag are shown in Fig. S2. The effect of exposing bacteria to light alone on the subsequent phage infection is shown in Fig. S3.

2.4 RNA extraction and RT-qPCR (reverse transcription quantitative PCR)

To probe ENMs' influence on bacterial gene regulation in relation to patterns of phage f1 infection, the expression of F-pili and membrane protein genes of *E. coli* K12 was assessed using RT-qPCR. 13.5 mL *E. coli* K12 suspension in LMW (OD_{600} = 0.4 ± 0.02) was treated with 1.5 mL n-TiO_2 P25, n-Ag, or their mixtures (cell-to-ENMs volume ratio of

Table 1 ENMs exposure experiment groups for phage infection

Group no.	ENMs	Final concentrations
1	n-TiO_2 P25	0, 0.02, 0.05, 0.1, 0.2, 0.5, 1, 2, 5, and 10 mg L^{-1}
2	n-Ag	0, 0.5, 1, 2, 5, 10, 20, 50, 100, 200, and 500 μg L^{-1}
3	n-TiO_2 P25 + n-Ag	n-TiO_2: 0, 0.1, 0.2, and 0.5 mg L^{-1} n-Ag: 0, 5, 10, 20, and 50 μg L^{-1}

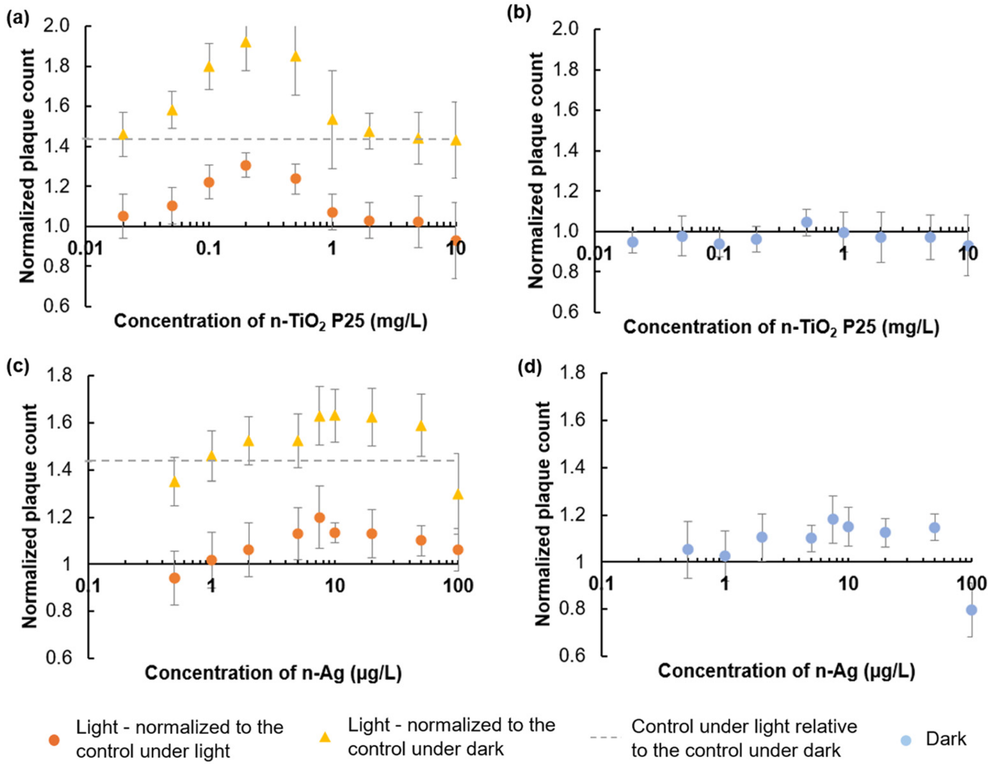

Fig. 2 Effects of sublethal concentrations of ENMs on phage f1 infection under light (a and c) and dark (b and d). The plaque counts of ENMs-free samples (control) under light or dark were set to 1 and the other results were normalized to the control as described in the legend.

9:1) with final concentrations listed in Table 1 group 3. Two sets of samples were prepared with one set wrapped with ultraclean film and exposed to the same light source mentioned above and the other set covered with aluminum foil to maintain dark conditions. All samples were mixed at 320 rpm and incubated for two hours.

The total RNA of each bacteria sample was extracted using the PureLink™ RNA Mini Kit (Invitrogen™) following the manufacturer's instructions and RNA concentration and quality were determined by micro-spectrophotometer (Eppendorf BioSpectrometer® and μCuvette®) analysis and gel electrophoresis. cDNA was synthesized using the High-Capacity cDNA Reverse Transcription Kit (Applied Biosystems™) following the manufacturer's protocol. RT-qPCR samples were prepared using the PowerTrack™ SYBR Green Master Mix for qPCR (Applied Biosystems™) and analysis was performed on a Bio-Rad CFX real-time PCR system. The targeted genes and primers are listed in Table S3. The qPCR thermal cycling was set according to the protocol of the SYBR Green Master Mix: enzyme activation at 95 °C for 2 min, followed by 40 cycles of denaturation at 95 °C for 15 s and annealing/extension at 60 °C for 60 s. The optimal cDNA input was determined by standard curves of targeted genes. The relative gene expression was calculated using the $2^{-\Delta\Delta Ct}$ method (Fold gene expression = $2^{-\Delta\Delta Ct}$, where $\Delta\Delta Ct = \Delta Ct$ (sample) − ΔCt (control) and $\Delta Ct = Ct$ (gene of interest) − Ct (housekeeping gene)). Ct of each gene was determined by taking the average of a minimum of three samples.

2.5 Physical mechanisms of ENMs affecting phage infection at the cell surface

Images of the ENMs and their mixtures at cell surface were captured using S/TEM and the sample preparation was modified from Han *et al.*[29] and Costa *et al.*[53] *E. coli* K12 suspension in LMW (OD_{600} = 0.4 ± 0.02) was exposed to 0.2 or 0.5 mg L^{-1} n-TiO_2 and/or 50 μg L^{-1} n-Ag, individually and in mixtures (cell-to-ENMs volume ratio of 9:1). Two sets of samples were prepared with one set wrapped with ultraclean film and exposed to the same light source mentioned before and the other set covered with aluminum foil in the dark. All samples were continuously mixed (200 rpm) and incubated for two hours. Then, phage f1 lysate was added to the mixtures (cell-to-phage volume ratio of 20:1) and mixed under dark for 1 hour. Samples were collected and fixed with 2.5% glutaraldehyde. Each sample was drop-cast to a glow-discharged formvar/carbon film 300 mesh copper grid (Electron Microscopy Sciences, FCF300-CU) and left for 4 minutes. The remaining mixture was then removed using filter paper. 2 μL of 2% phosphotungstic acid was applied to stain each sample for 30 seconds and removed. The staining procedure was repeated 3 times to ensure sufficient and even staining. After drying, grids with bacteria and phage samples were stored and examined with a Hitachi HD-2300A Dual EDS S/TEM system.

Aggregate sizes of n-TiO_2 in dark and n-TiO_2 + n-Ag mixtures with and without light exposure were measured using Nano Zetasizer (Malvern Instruments Ltd) under the same experimental conditions in LMW. The concentration range of n-Ag applied in the experiment is below the limit (0.01 mg mL^{-1} for size smaller than 10 nm) of the instrument and therefore, the aggregate size of n-Ag was not measured. Zeta potential of n-TiO_2 and n-Ag, individually and in mixtures (concentrations listed in Table 1 group 3), in LMW exposed to light and dark for 2 hours was measured by Nano Zetasizer (Malvern Instruments Ltd). Two measurements of each parameter were taken. The average aggregate sizes are shown in Fig. S11, and average zeta potential is shown in Fig. S12.

2.6 Data analysis

Pearson's correlation coefficient was calculated to determine whether OMP and phage infection after exposure to ENMs or their mixtures are positively or negatively related, as well as the strength of the relationship. Non-metric multidimensional scaling (NMDS) plots were generated by condensing the multidimensional data set (*i.e.*, relative expression of targeted genes) into a 2D representation to show the association between select genes (Table S3) under ENM exposure through similarity/dissimilarity between data. Pearson's correlation coefficient and NMDS plots were generated using R, and the results are shown in SI (Table S4, Fig. S4 and S7).

Heat maps for relative gene expression were created with Excel (Fig. 4 and 5 and S6). All markers or bar columns with error bars represent "mean ± SD (standard deviation)" in the charts (Fig. 2–4 and S2, S3, S5 and S6).

3 Results and discussion

3.1 Effects on phage infection

3.1.1 Sublethal doses of photoactive ENMs promote phage infection under light. Previously we found that photoactive ENMs (*e.g.*, n-TiO_2, n-Ag, *etc.*) induced significant sublethal bacterial stress, reflected by an increase in OMP, at environmentally relevant doses (<1 mg L^{-1}) in freshwater with simulated sunlight irradiation.[41] To investigate if this outer membrane damage translates to greater phage infection of *E. coli*, we employ the same experimental conditions and measure the phage f1 infection at low ENM doses in the presence and absence of light by plaque counts and normalized to ENMs-free samples as shown in Fig. 2.

Under light, initial exposure of *E. coli* to ENMs results in a 25% increase in phage infection with 0.2 mg L^{-1} n-TiO_2 (Fig. 2a – orange symbols) and a 20% increase with 7.5 μg L^{-1} n-Ag (Fig. 2c – orange symbols), compared to the no-ENM control under light. Relative to the no-ENM control under dark, there is a 75% increase in phage infection with 0.2 mg L^{-1} n-TiO_2 (Fig. 2a – yellow symbols) and a 68% increase with 7.5 μg L^{-1} n-Ag (Fig. 2c – yellow symbols). As illustrated in Fig. 2a and c, the relative phage infection levels increase as the concentration of individual ENMs increase, reaching a maximum, and then decrease at higher concentrations. The results follow trends similar to the ENM effects on cell OMP,[41] indicating that the increased bacterial OMP, induced by low doses of ENMs under light, may facilitate the infection process of phage f1. The Pearson's correlation coefficient (Table S4) also confirms the positive correlation between OMP, from our previous work conducted under the same experiment conditions,[41] and phage infection. *E. coli* pre-treated with light alone shows a 40% increase in phage infection compared to the samples without light treatment as illustrated in Fig. S3. Previously, we observed a 20–40% increase in cell OMP with only light exposure.[41] Thus, the results further demonstrate that the presence of ENMs amplifies the effects of light on phage infection, and that increased phage infection follows increased OMP when exposed to either light alone or ENMs under light. The same conclusion was also drawn by Xiao *et al.*[30] when they exposed phage/bacteria (engineered phage M13 and *E. coli* TG1) suspension to 0.5 mM n-TiO_2 under UV irradiation (365 nm, 150 μW cm^{-2}) and observed increases in both bacteria OMP

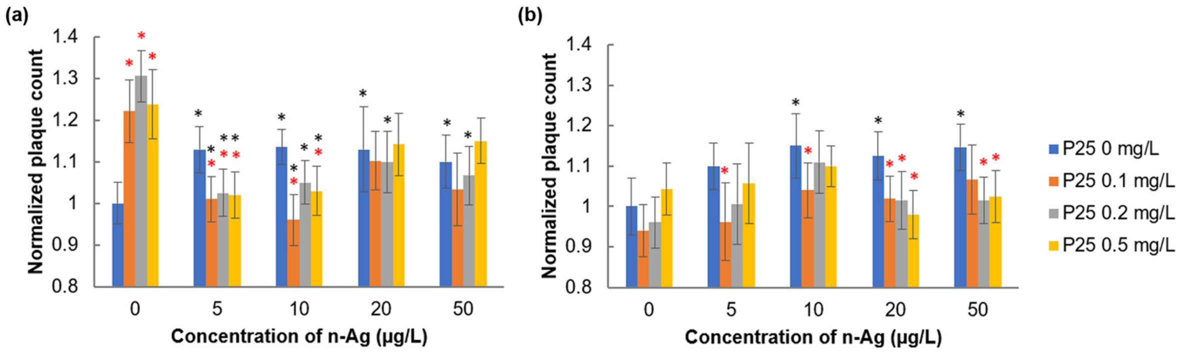

Fig. 3 Effects of low concentrations of n-TiO_2 + n-Ag mixtures on phage f1 infection: (a) under simulated sunlight and (b) under dark. The plaque counts of ENMs-free samples (control) under light or dark were set to 1 and the corresponding treatment results were normalized to the control. Statistical significance ($p < 0.05$) for values compared with the corresponding concentration of n-Ag (without n-TiO_2) and n-TiO_2 (without n-Ag) is indicated by red and black asterisks, respectively. P25 = n-TiO_2 P25.

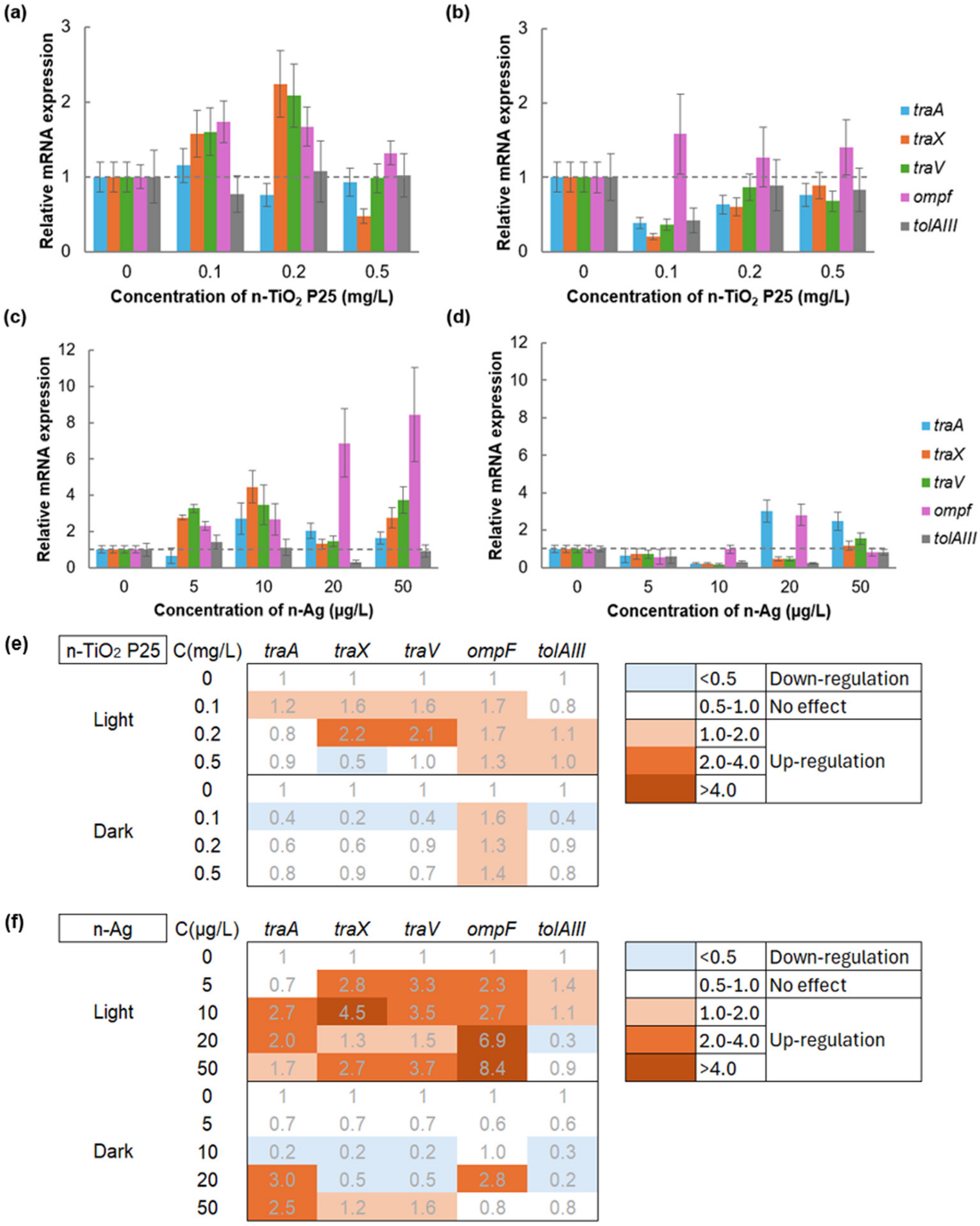

n-TiO2 P25	C(mg/L)	*traA*	*traX*	*traV*	*ompF*	*tolAIII*
	0	1	1	1	1	1
Light	0.1	1.2	1.6	1.6	1.7	0.8
	0.2	0.8	2.2	2.1	1.7	1.1
	0.5	0.9	0.5	1.0	1.3	1.0
	0	1	1	1	1	1
Dark	0.1	0.4	0.2	0.4	1.6	0.4
	0.2	0.6	0.6	0.9	1.3	0.9
	0.5	0.8	0.9	0.7	1.4	0.8

	<0.5	Down-regulation
	0.5-1.0	No effect
	1.0-2.0	Up-regulation
	2.0-4.0	
	>4.0	

n-Ag	C(µg/L)	*traA*	*traX*	*traV*	*ompF*	*tolAIII*
	0	1	1	1	1	1
	5	0.7	2.8	3.3	2.3	1.4
Light	10	2.7	4.5	3.5	2.7	1.1
	20	2.0	1.3	1.5	6.9	0.3
	50	1.7	2.7	3.7	8.4	0.9
	0	1	1	1	1	1
	5	0.7	0.7	0.7	0.6	0.6
Dark	10	0.2	0.2	0.2	1.0	0.3
	20	3.0	0.5	0.5	2.8	0.2
	50	2.5	1.2	1.6	0.8	0.8

	<0.5	Down-regulation
	0.5-1.0	No effect
	1.0-2.0	Up-regulation
	2.0-4.0	
	>4.0	

Fig. 4 Effects of low concentrations of n-TiO_2 or n-Ag on *E. coli* genes expression under light (a and c) and dark (b and d). The dash lines mark the reading of 1, which is the relative mRNA expression of no-ENMs control under light or dark (the first set of bars). A value of 0.5–1 indicates no significant change compared to the control. (e) and (f) are heatmaps. C = ENM concentration.

and phage transduction. High concentrations of ENMs (*e.g.*, n-TiO_2, n-Ag,[20] and nZVI[16–18]) reduce cell viability and may also inactivate phages, which leads to the reduced ENMs effects on phage infection beyond the maximum sublethal effects in Fig. 2a and c.

Under dark, prior exposure to n-TiO_2 has no effect on phage infection (Fig. 2b). However, slight increases in phage infection are observed in bacteria samples pre-treated with 5–50 µg L^{-1} n-Ag (Fig. 2d). Our previous results showed that n-TiO_2 or n-Ag exerted minimal effect on OMP in the dark.[41] The results in Fig. 2d suggest that exposure to n-Ag in dark may increase phage infection through pathways other than increased OMP, such as bacterial stress related to Ag^+ release due to oxidative dissolution of n-Ag.[54] In addition, the Ag^+ cation may enhance the attachment of phage to cell surface through electrostatic effects, reducing the repulsive charge barrier between phage and cell.[55] Previous research has reported that exposure of phage and other viruses to n-Ag prior to infection can facilitate the process, although n-Ag has negative impacts on the viral genetic material production after infection.[22,56] Zhang *et al.*[23] observed phage-mediated attachment of n-Ag to bacteria that might contribute to the promoting effect of n-Ag on phage infection. They suggested that negatively charged n-Ag binds to the positively charged pVIII protein which encapsulates the DNA of filamentous phage. In this way, the phage carries n-Ag to the host cell

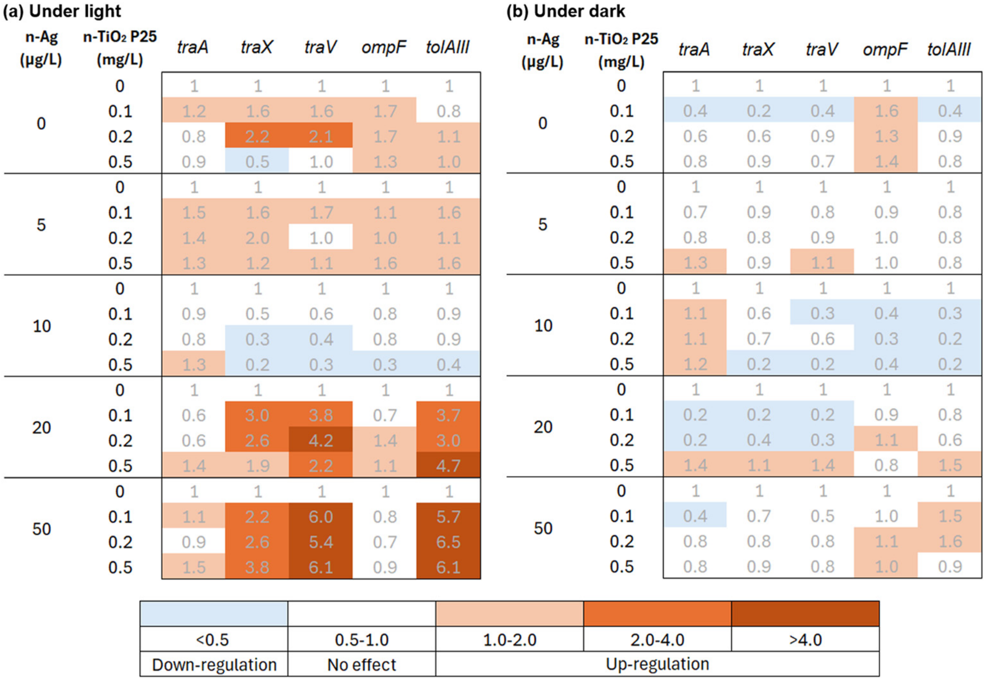

(a) Under light

n-Ag (μg/L)	n-TiO₂ P25 (mg/L)	*traA*	*traX*	*traV*	*ompF*	*tolAIII*
0	0	1	1	1	1	1
	0.1	1.2	1.6	1.6	1.7	0.8
	0.2	0.8	2.2	2.1	1.7	1.1
	0.5	0.9	0.5	1.0	1.3	1.0
5	0	1	1	1	1	1
	0.1	1.5	1.6	1.7	1.1	1.6
	0.2	1.4	2.0	1.0	1.0	1.1
	0.5	1.3	1.2	1.1	1.6	1.6
10	0	1	1	1	1	1
	0.1	0.9	0.5	0.6	0.8	0.9
	0.2	0.8	0.3	0.4	0.8	0.9
	0.5	1.3	0.2	0.3	0.3	0.4
20	0	1	1	1	1	1
	0.1	0.6	3.0	3.8	0.7	3.7
	0.2	0.6	2.6	4.2	1.4	3.0
	0.5	1.4	1.9	2.2	1.1	4.7
50	0	1	1	1	1	1
	0.1	1.1	2.2	6.0	0.8	5.7
	0.2	0.9	2.6	5.4	0.7	6.5
	0.5	1.5	3.8	6.1	0.9	6.1

(b) Under dark

n-Ag (μg/L)	n-TiO₂ P25 (mg/L)	*traA*	*traX*	*traV*	*ompF*	*tolAIII*
0	0	1	1	1	1	1
	0.1	0.4	0.2	0.4	1.6	0.4
	0.2	0.6	0.6	0.9	1.3	0.9
	0.5	0.8	0.9	0.7	1.4	0.8
5	0	1	1	1	1	1
	0.1	0.7	0.9	0.8	0.9	0.8
	0.2	0.8	0.8	0.9	1.0	0.8
	0.5	1.3	0.9	1.1	1.0	0.8
10	0	1	1	1	1	1
	0.1	1.1	0.6	0.3	0.4	0.3
	0.2	1.1	0.7	0.6	0.3	0.2
	0.5	1.2	0.2	0.2	0.4	0.2
20	0	1	1	1	1	1
	0.1	0.2	0.2	0.2	0.9	0.8
	0.2	0.2	0.4	0.3	1.1	0.6
	0.5	1.4	1.1	1.4	0.8	1.5
50	0	1	1	1	1	1
	0.1	0.4	0.7	0.5	1.0	1.5
	0.2	0.8	0.8	0.8	1.1	1.6
	0.5	0.8	0.9	0.8	1.0	0.9

<0.5	0.5-1.0	1.0-2.0	2.0-4.0	>4.0
Down-regulation	No effect	Up-regulation		

Fig. 5 Heatmaps of *E. coli* gene expression with exposure to low concentrations of n-TiO_2 + n-Ag mixtures under light (a) and dark (b), relative to n-Ag-only control. Bar charts with standard deviation are shown in Fig. S5.

and further facilitates phage infection. It is noteworthy that although capping and stabilizing agents like citrate, as used in this study, may influence the kinetics of n-Ag dissolution and aggregation through complexation,[57] we nonetheless observe the sublethal stress of n-Ag on bacteria[41] and phage infection, consistent with the results in other studies where significant cellular or phage responses were not suppressed or affected by citrate-stabilized n-Ag.[20,58]

3.1.2 ENM mixtures suppress the effects of individual ENMs on phage infection. Low concentrations of n-TiO_2 + n-Ag mixtures can exert synergistic bacterial stress under light (*e.g.*, decreased ATP levels and damaged cell membranes) due to increased ROS production.[42] Our previous findings also illustrated that under simulated sunlight irradiation, n-TiO_2 + n-Ag mixtures at environmentally relevant concentrations synergistically induce greater OMP (up to 72–102% more) than that caused by individual ENMs.[41] Thus, we expected to observe a similar enhancement in phage infection induced by the ENM mixtures under the same experimental conditions. However, the results, presented in Fig. 3, show an overall attenuation of phage infection by n-TiO_2 + n-Ag mixtures, reflecting a trend counter to their effects on OMP and in contrast to the effects of n-TiO_2 or n-Ag alone.

In Fig. 3a, under light at lower n-Ag doses (5–10 μg L^{-1}), bacterial exposure to n-TiO_2 + n-Ag mixtures generates phage infections similar to the no-ENM illuminated control, around 20–30% less than being exposed to n-TiO_2 alone (the first set of bars with no n-Ag) and about 13% less than being exposed to n-Ag alone (the blue bars). At 20–50 μg L^{-1} n-Ag, phage infections induced by exposure to n-TiO_2 + n-Ag mixtures increase slightly (1.1-fold) relative to the control without ENMs, around 5–20% less than being exposed to n-TiO_2 alone (the first set of bars with no n-Ag) and at similar levels relative to exposure to n-Ag alone (the blue bars). Under dark in Fig. 3b, there is no significant difference between the phage infection of bacteria exposed to n-TiO_2 + n-Ag mixtures and the results of no-ENMs control (the first blue bar) or exposure to n-TiO_2 alone (the first set of bars with no n-Ag). A slight reduction (<13%) in phage infection is observed with exposure to the ENM mixtures compared to the results of n-Ag alone (the blue bars). In contrast, then, to the measurable positive effects on phage infection exerted by n-TiO_2 or n-Ag alone under light and by n-Ag in the dark (Fig. 2), under light the ENM mixtures suppress phage infection and this suppression lessens with increasing n-Ag dose in the mixtures; under dark the ENM mixtures suppress the positive effects of n-Ag alone on phage infection. In other words, the interactions between the ENMs of the mixtures are antagonistic or result in effects less than the addition of the individual ENM effects.

In Table 2, we summarize qualitatively the relationship between OMP increase[41] and phage infection (Fig. 2 and 3) induced by low doses of n-TiO_2, n-Ag, and their mixtures. When exposed to n-TiO_2, we observe increases in both OMP and phage infection under light and no effects in either measurement under dark. When exposed to n-Ag, both OMP and phage infection increase under light. Under dark, there is no effect on OMP, but we observe slight increases in phage infection, which we attribute to the oxidative dissolution of n-Ag to release Ag^+ ions.

Table 2 A qualitative summary of the effects of n-TiO_2, n-Ag, and their mixtures on bacterial OMP and phage infection

	Under SSI		Under dark	
ENM types	OMP	Phage infection	OMP	Phage infection
n-TiO_2	+	+	0	0
n-Ag	+	+	0	+
n-TiO_2 + n-Ag	+++	-[a]	0	-[a]

Note: "+" represents a promoting effect, "0" represents no effect, and "-" represents a suppressing or inhibiting effect. OMP = outer membrane permeability.[a] The ENM mixtures suppressed the effects exerted by ENMs individually. Compared to the no-ENM control, they caused negligible effects on phage infection.

When exposed to the binary ENM mixtures under light, there is a large increase in OMP but slightly suppressing (at low n-Ag concentrations) to negligible effect on phage infection. Under dark conditions, there is slight suppression in phage infection with exposure to the ENM mixtures relative to the effects caused by n-Ag alone under dark and no significant difference relative to the no-ENM control on either measurement under dark. The negative correlation between OMP and phage infection is also indicated by the Pearson's correlation coefficient (Table S4).

These results reveal that ENMs have variable effects on phage–host interactions. Sublethal stress exerted by individual photoactive ENMs under light, likely associated with ROS generation, increases OMP and boosts phage entry into the periplasmic space where the phage binds to the TolA protein (Fig. 1c). Under dark conditions, n-Ag undergoes oxidative dissolution to release Ag^+ which has a positive effect on phage infection, unrelated to increased OMP. The Ag^+ ion may exert favorable electrostatic effects to reduce charge repulsion and enhance phage–bacterial interactions (Fig. S11), or the dissolved silver cations may cause bacterial stress in other ways that make the bacteria more susceptible to phage infection.[22] Under light conditions, the net effect of n-Ag dissolution on phage infection is reduced due to photoreduction of Ag^+ back to Ag^0.[42]

ENM mixtures, however, cause even greater damage to the outer membranes of *E. coli* but without a concomitantly positive effect on phage infection. Thus, we propose that illuminated ENM mixtures impair some aspects of the complex sequence of events involved in phage infection (Fig. 1) beyond outer membrane damage (increased OMP which allows phage entry into the periplasmic space). Since, under light, released Ag^+ ions adsorb to n-TiO_2 and are photoreduced to Ag^0, forming a new nanocomposite (Fig. 6f and S10) that produces more ROS and exerts greater phototoxicity,[42] damage to membrane proteins critical to phage infection such as TolA may accompany the greater OMP increase caused by the ENM mixtures. Under dark, strongly adsorptive n-TiO_2 sorbs released Ag^+, reducing its effect on phage infection observed with exposure to individual n-Ag in the dark.[59–62] The interactions between n-Ag and n-TiO_2 under light and dark and under the same experimental conditions were examined (*e.g.*, extracellular ROS generation, dissolved Ag^+ concentration, adsorption to n-TiO_2, and ATP levels) and discussed in detail in previous studies.[42,62] Subsequent experiments, discussed below, probe the various effects that ENM exposure exerted on the complex interactions controlling phage entry into the bacterial cell to explain these differing observations.

3.2 Effects on the expression of F-pili and membrane protein genes

Exposure to ENMs can alter the expression of genes involved in the mechanism of phage infection.[63] Previous studies showed that n-TiO_2 can stimulate F-pili-related genes that assist in the infection process of filamentous phages (Fig. 1a), and exposure to n-TiO_2 with UV irradiation had a synergistic effect on increasing F-pili gene expression as well as phage transduction.[29,30] To investigate the relationships between ENM exposure, OMP, phage infection, and the expression of key genes involved in phage entry into the bacterial cell, we conduct RT-qPCR to measure transcription of genes for specific cellular structures and proteins associated with the early events of filamentous phage binding at the cell surface (Fig. 1) as a function of exposure to n-TiO_2 and n-Ag and their mixtures under light and dark. Using *rpoA* as the housekeeping gene, we quantify the RNA transcripts for three F-pili-related genes: *traA* for encoding the pilin precursor, *traX* for pilin acetylation, and *traV* for pilus assembly.[29,30] Additionally, we quantify expression of the *ompF* gene that encodes the outer membrane protein OmpF, which may serve as a receptor and/or assist phage entry to cells.[46,64] We also measure the expression of *tolAIII* gene, encoding the third domain of the periplasmic protein and receptor, TolA.[47] The possible scenarios of the infection process of filamentous phages like phage f1 and the functions of F-pili and the membrane proteins are summarized in detail in Fig. 1. Our goal is to investigate the patterns of gene expression relative to OMP and phage infection to gain greater insight about how damage to cell surface structures by ENMs is related to the stimulation or disruption of key steps in the complex sequence of events involved in phage entry into the cell.

3.2.1 Gene expression regulated by photoactive ENMs under light. Fig. 4 shows the relative expression of targeted genes in *E. coli* exposed to sublethal doses of n-TiO_2 or n-Ag under light and dark. When exposed to n-TiO_2 under light, the expression of F-pili-related genes, particularly *traX* and *traV*, increases 60–124% at 0.1–0.2 mg L^{-1} n-TiO_2 compared to the no-ENMs control under light, the *ompF* gene expression increases 32–74%, and the *traA* and *tolAIII* gene expression shows no significant change (Fig. 4a and e). Under dark, exposure to n-TiO_2 induces negligible effects on the expression of all tested genes, except a slight down-regulation in the expression of *traA*, *traX*, *traV*, and *tolAIII* genes at 0.1 mg L^{-1} n-TiO_2 and slight up-regulation of the *ompF* gene at 0.1–0.5 mg L^{-1} n-TiO_2 (Fig. 4b and e).

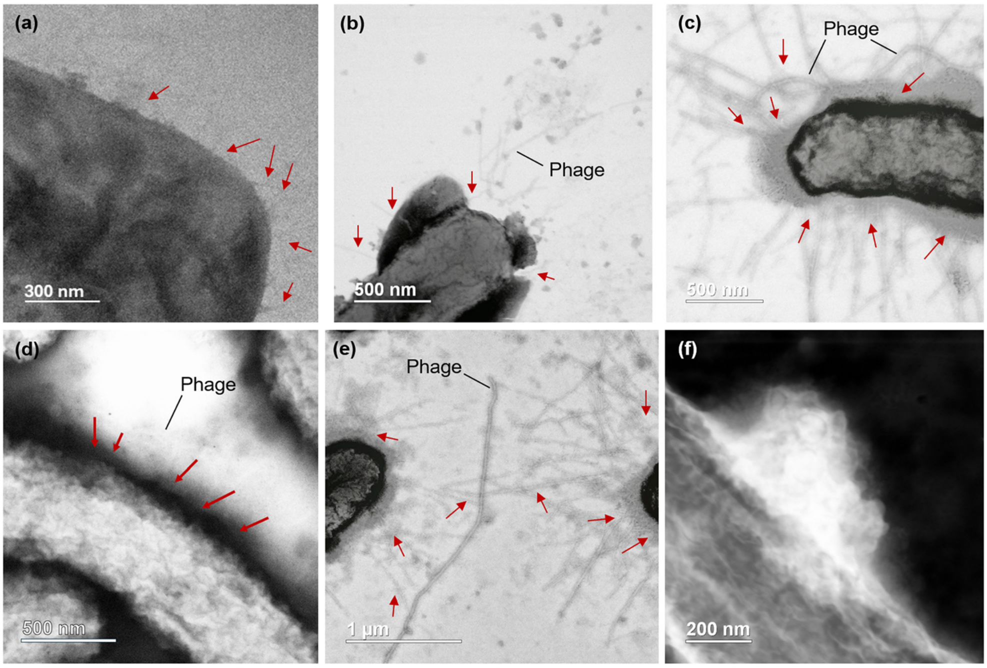

Fig. 6 S/TEM images of *E. coli* pre-treated with ENMs under light and infected with phage f1: (a) control without ENMs, (b) exposed to 0.2 mg L^{-1} n-TiO$_2$, (c) exposed to 50 μg L^{-1} n-Ag, (d) exposed to 0.2 mg L^{-1} n-TiO$_2$ + 5 μg L^{-1} n-Ag mixture, and (e) and (f) exposed to 0.2 mg L^{-1} n-TiO$_2$ + 50 μg L^{-1} n-Ag mixture. Fig. 6a–e are in light field TE mode and Fig. 6f is in dark field TE mode, showing the attachment of the ENM mixtures on cell surface (EDS analysis provided in Fig. S10). The red arrows point to the pili/F-pili on bacteria, which are faint and relatively difficult to observe in Fig. 6a, b and d.

When the bacteria are stressed by n-Ag and light, we notice significant increases in the expression of various genes at different n-Ag concentrations (Fig. 4c and f). When exposed to 5–10 μg L^{-1} n-Ag, we see a major increase, 1.3-to-3.5-fold, in the expression of *traX* and *traV* genes relative to the no-ENMs control, and smaller increases around 1.7-fold in the *traA* gene expression (with 10 μg L^{-1} n-Ag) and 1.4–1.6-fold in the *ompF* gene expression. When exposed to 20–50 μg L^{-1} n-Ag, the *ompF* gene expression increases dramatically, 5.9-to-7.4-fold compared to the control, and the F-pili-related genes expression increases 0.7–2.7-fold. No effect is observed in the *tolAIII* gene expression when exposed to n-Ag alone under light. Under dark (Fig. 4d and f), no increase in gene expression is observed with exposure to 5–10 μg L^{-1} n-Ag. An increase of 2- and 1.8-fold relative to the control is detected in the expression of *traA* and *ompF* genes, respectively, with 20 μg L^{-1} n-Ag added, and a slight increase of 1.5- and 0.6-fold relative to the control is detected in the expression of *traA* and *traV*, respectively, with exposure to 50 μg L^{-1} n-Ag under dark. The *tolAIII* gene expression shows slight suppression or negligible change when exposed to n-Ag alone under dark.

Table 3 lists the qualitative effects of the two ENMs on OMP,[41] phage infection, and the expression of select genes, summarizing the results in Fig. 2 and 4, to better understand qualitatively how patterns of select gene expression align with changes in OMP and phage infection under the conditions of this study. Previous studies have demonstrated a corresponding relationship between enhanced expression of *traA*, *traX*, and *traV* genes and increased filamentous phage transduction in response to n-TiO$_2$-induced intracellular ROS production at much higher

Table 3 A qualitative summary of the effects of n-TiO$_2$ and n-Ag on OMP, and phage infection, and the expression of select genes

		Under SSI		Under dark	
Genes related to phage infection		n-TiO$_2$	n-Ag	n-TiO$_2$	n-Ag
OMP		+	+	0	0
Phage infection		+	+	0	+
F-pili-related genes	*traA*	0	+	0/-	0/+
	traX	+	+	0/-	0/-
	traV	+	+	0/-	0/-
Membrane protein genes	*ompF*	+	++	0/+	+
	tolAIII	0	0	0	0/-

Note: "+" represents a promoting effect, "0" represents a negligible or no significant effect, and "-" represents down-regulation. OMP = outer membrane permeability.

doses (0.05–50 mM or 4 mg L^{-1}–4 g L^{-1}).[29,30] Similarly, our results show that bacteria exposed to much lower concentrations of n-TiO_2 (0.1–0.5 mg L^{-1}) and n-Ag (5–50 μg L^{-1}) under light exhibit higher levels of relative mRNA expression of F-pili-related genes, especially the *traX* and *traV* genes that acetylate and assemble F-pili and may facilitate phage infection. NMDS plots also indicate high similarity and thus, strong association between *traX* and *traV* gene expression data based on the relative position of the centroids and data point clusters in Fig. S4. Since F-pili assist with phage-to-cell contact and the expression of *traA*, *traX*, and *traV* genes promote F-pili formation,[53,65,66] we propose that in addition to increasing OMP,[41] n-TiO_2 and n-Ag at environmentally relevant concentrations under light irradiation stimulate F-pili gene expression, likely due to ROS generation that triggers a cellular stress response, which promotes F-pili formation and phage-to-cell contact, and ultimately enhances phage infection. It is noted that exposure to n-Ag induces an overall higher level of gene expression than n-TiO_2 under light, which may be attributed to the greater toxicity of n-Ag through mechanisms of particle-specific antimicrobial properties and released Ag^+ which enters the cell more easily.[67] The expression of *traA* gene for F-pili encoding is promoted slightly only by n-Ag under both light and dark conditions, indicating that *traA* gene expression may be facilitated by Ag^+ released from n-Ag under light and dark, and may contribute to phage infection under these conditions (Table 3).

However, the expression of membrane protein genes may not be the major factor in how individual ENMs affect phage infection in this study. As shown in Table 3, no increase in phage infection is observed when exposed to n-TiO_2 under dark even though *ompF* gene expression increased, and the effect of n-Ag on phage infection increase is not enhanced in a pattern commensurate with the dramatic elevation of the *ompF* gene expression at 20–50 μg L^{-1} n-Ag under light (Fig. 1c and 3c). In addition, the *tolAIII* gene expression is either unchanged or slightly down-regulated when exposed to n-TiO_2 or n-Ag under light or dark (Table 3). The far distance between the ordinates of *ompF* or *tolAIII* gene expression data centroid and the data point clusters in the NMDS plot in Fig. S4 also indicate weak association between these two genes and the F-pili-related genes. These observations suggest that 1) the periplasmic protein TolA, integral to filamentous phage infection, is not stressed, damaged, or stimulated by either of the two ENMs individually under these experimental conditions, and 2) there are alternate routes to pass through the outer membrane, not involving the outer membrane protein, OmpF, that the *ompF* gene encodes (Fig. 1c), as the expression of the two membrane proteins does not track the patterns of ENMs' effects on OMP or phage infection.

As mentioned previously, the outer membrane protein, OmpF, is associated with the outer membrane transport[45,68] and it also serves as a receptor for certain phages, including phages λ, K20, Tu1a, and T2.[69] The increased OMP or lipid peroxidation caused by ENMs may allow phage entry to the periplasmic space to activate the receptors (related to TolA and other Tol–Pal proteins) on the cytoplasmic membrane to complete the infection process,[41,45,70] possibly bypassing the OmpF protein (Fig. 1c). The up-regulation of the *ompF* gene with exposure to n-TiO_2 under light and slightly under dark (especially in comparison to down-regulation or no change of most of the other tested genes) and n-Ag under light and dark suggests possible triggers related to ENM-induced ROS generation (under light),[71] released Ag^+,[54] and physical attachment of ENMs (under dark). There are dramatic increases in the *ompF* gene expression with n-Ag exposure under light and the effect is amplified with increasing n-Ag concentrations, suggesting a cumulative result from all pathways – ROS generation,[72,73] released Ag^+ caused by n-Ag dissolution,[54] and attachment of n-Ag on the cell surface.[67] Although there is an overlap between causes of *ompF* gene stimulation and mechanisms of OMP increase,[41] our findings suggest little to no association between *ompF* gene expression and phage infection under the stress from n-TiO_2 or n-Ag which can be explained by the outer-membrane-damage-induced phage entry.

3.2.2 Synergistic regulation of gene expression by the ENM mixtures under light. When bacteria are exposed to n-TiO_2 + n-Ag mixtures in the dark, the expression of select genes mostly shows no change or down-regulation, except under a few conditions, relative to the control group treated by n-Ag only (Fig. 5). In Fig. 5a under light, slight increases (33–53%) are observed in the *traA* gene expression of samples exposed to ENM mixtures at low n-Ag concentration (5 μg L^{-1}, all n-TiO_2 levels) or higher n-TiO_2 concentration (0.5 mg L^{-1}, all n-Ag levels) compared to the n-Ag-only control. In contrast, we observe striking increases in the expression of *traX* (0.9-to-2.7-fold), *traV* (1.2-to-5.0-fold) as well as *tolAIII* (1.9-to-5.5-fold) genes at higher concentrations of n-Ag (20–50 μg L^{-1}) and all n-TiO_2 concentrations. The *ompF* gene expression shows slight increases (35–56%), almost insignificant, compared to the n-Ag-only control.

The patterns in the gene expression data are more amplified and show greater statistical significance under light when we analyze the data by comparing to control samples in the absence of ENMs (Fig. S6). Clearly, at higher concentrations of n-Ag (20–50 μg L^{-1}) under light, the effects of the ENM mixtures on the expression of these genes are greater than the sum of effects of n-TiO_2 and n-Ag acting alone. For example, 20 μg L^{-1} n-Ag induces a 0.5-fold increase in the expression of *traV* gene under light (Fig. 4c and f), and 0.2 mg L^{-1} n-TiO_2 induces a 1.1-fold increase (Fig. 4a and e). When exposed to 20 μg L^{-1} n-Ag + 0.2 mg L^{-1} n-TiO_2 mixture under light, an increase of 5.1-fold is reached in the same gene expression (Fig. S6-e and m). Under dark, the results show negligible changes compared to the no-ENM control, except for very few cases presented in Fig. S6-b, h and n.

In Table 4, we summarize qualitatively the effects of the binary ENM mixtures on OMP,[41] phage infection (Fig. 3), and gene expression (Fig. 5 and S6) to identify trends among these phenomena. Our results (Fig. 5) reveal

Table 4 A qualitative summary of the effects of the ENM mixtures on cell OMP, phage infection, and the expression of select genes

		ENM mixtures under SSI		ENM mixtures under dark	
Phenomena		Compared to n-Ag	Compared to no-ENMs	Compared to n-Ag	Compared to no-ENMs
OMP		++	+++	0	0
Phage infection		-	0	-	0
F-pili-related genes	*traA*	0	+	0	+
	traX	++	+++	0	0
	traV	++	+++	0	0
Membrane protein genes	*ompF*	0	+++	0	+
	tolAIII	++	+++	0	0

Note: "+" represents a promoting effect, "0" represents negligible or no significant effect, and "-" represents a suppressing/inhibiting effect. OMP = outer membrane permeability.

significant up-regulation of certain tested genes (*e.g.*, *traX*, *traV* and *tolAIII*) with exposure to n-TiO_2 + n-Ag mixtures at certain concentration ranges (*e.g.*, 20–50 μg L^{-1} n-Ag) under light. NMDS plots (Fig. S7) showing clusters with respect to n-Ag concentration range under light and the high similarity between *traX*, *traV*, and *tolAIII* gene expression data also confirm our observations from a statistical perspective.

The up-regulation of genes under light, especially at high n-Ag concentrations, aligns with increased OMP but does not correspond to greater phage infection (Fig. 3). In fact, the phage infection is suppressed or shows negligible differences relative to individual ENM controls, despite enhanced ROS production under light as evidenced in previous research,[30,42] elevated OMP,[41] and synergistic effects on gene expression. This can be attributed to a variety of factors associated with the formation of the more phototoxic n-Ag/n-TiO_2 composite (Fig. 6f and S10) that produces more ROS and may inactivate phages,[74] cause greater damage to F-pili or critical membrane proteins, disrupt normal bacterial functions, and/or physically interfere with phage–cell contact. The fact that the *tolAIII* gene expression is stimulated significantly with exposure to n-TiO_2 + n-Ag mixtures under light (Fig. 5 and S6) but is otherwise unaffected under conditions of individual ENM exposure (Fig. 4) suggests that the greater level of ROS generation goes beyond damage to outer membranes and impairs the periplasmic protein, TolA. Although *tolAIII* gene expression can be regulated by other mechanisms, such as the fumarate and nitrate reductase (*fnr*) gene in response to oxygen levels,[75] in our experiments oxygen levels are unchanged and thus, it is logical to attribute the up-regulation of the *tolAIII* gene to TolA damage. Metal ENMs, such as n-TiO_2, n-Ag, n-Au, and n-ZnO, have been shown to up-regulate genes related to cellular components or metabolism in bacteria,[76] zebrafish,[77,78] and mice[79,80] as a response to oxidative stress or stress-induced inflammation and apoptosis. Based on our results, we propose that the binary ENM mixtures cause severe sublethal stress to cells such as damaging periplasmic membrane proteins to suppress phage infection. At the same time, this damage activates repair processes (*e.g.*, SOS response) as reflected by the stimulated gene expression at higher concentrations of n-Ag (>20 μg L^{-1}) under light which lessens or offsets the inhibitory effects on phage infection observed at lower n-Ag concentrations and all concentrations in the dark (Fig. 3).

The fact that the relative expression level of *ompF* with exposure to the ENMs mixtures exhibits significant increase compared to no-ENMs control (Fig. S6) while unchanged compared to n-Ag-only control (Fig. 5 and Table 4) supports the previous discussion about *ompF* gene stimulation associated with released Ag^+ from n-Ag and ENM attachment to the cell surface. The trend does not follow the patterns of ENM effects on phage infection further confirms the alternate phage entry into the periplasmic space that bypasses the OmpF protein that the *ompF* gene encodes (Fig. 1c).

3.3 Effects on cell surface properties related to phage–cell contact

In addition to increasing OMP, ENMs are reported to alter other biophysicochemical properties of bacterial cell surface, such as F-pili density and surface charge, which may affect phage–cell contact and ultimately influence phage entry and infection rates.[22,33] Our results show up-regulation of F-pili-related genes, specifically *traX* (for acetylation) and *traV* (for assembly), induced by n-TiO_2, n-Ag, and their mixtures under light (Fig. 4 and 5). To further investigate these phenomena, specifically F-pili density and phage–cell contact, we image *E. coli* cells pre-treated with n-TiO_2 and n-Ag and their mixtures under light and infected by phage f1 (Fig. 6) using S/TEM. In addition, we measure the zeta potential of the ENMs and their mixtures under light and dark (Fig. S11) to investigate how ENMs may modify electrostatic interactions at the bacterial surface.

Bacterial cells are covered with pili (thin, hair-like structures) for adhesion, among which the F-pili, also referred to as the sex or conjugation pili, are fewer, with a number of 1–4, thicker, and longer than the general pili.[81] They can extend up to 20 μm (ref. 82) and play a significant role in connecting the donor and recipient cells in conjugation (Fig. S8), as well as recognizing filamentous phage and promoting phage–host interaction as mentioned previously.[45] When exposed to ENMs under light, particularly n-Ag (50 μg L^{-1}) and the binary ENM mixtures at higher n-Ag concentration, and in comparison to the no-ENM control under light in Fig. 6a, other pre-treated samples (with n-TiO_2 and the binary ENM mixtures with low n-Ag concentration) in Fig. 6b and d, and samples exposed to the same doses of ENMs under dark in Fig. S9, there is a noticeable increase in the pili/F-pili density on the cell surface which may be facilitated by ENMs, observed to approach or bind to a nearby phage, as shown in Fig. 6c and e. Under dark, there are no visible differences in the pili density among all samples, with or without ENMs (Fig. S9).

Our findings are supported by previous studies where a correlation between enhanced F-pili-related gene expression and increased phage infection associated with the exposure to n-TiO_2 was reported.[29,30] It has been reported that up-regulation of F-pili-related genes and increased pili density may be associated with not only enhanced phage entry into the cell but also a stress response of the host cell,[83,84] which explains the increased pili/F-pili density with exposure to the binary ENM mixtures that induce more ROS damage to the cell (Fig. 6e).

We also observe ENMs, especially the binary ENM mixtures, accumulating and attaching to the cell surface (Fig. 6f and S10), which may affect phage infection in additional ways. On one hand, ENMs at low concentrations form smaller aggregates than at high concentrations (Fig. S11-a), and therefore, have higher mobility and relative surface area, exhibiting higher activity which may contribute to their effects on OMP[41] and phage infection (Fig. 2). The complex interactions between different entities of the ENMs-bacteria–phage system can also influence the aggregation behavior of ENMs and in turn, affect their toxicity and ecological impacts. For example, Zhang *et al.*[23] revealed that the biological binding, mediated by phage-specific recognition, between n-Ag and phage facilitated the aggregation of n-Ag (0.1 mg L^{-1}) on the host cell surface upon phage infection, which caused further ENMs-induced oxidative stress and outer membrane destabilization that promoted phage infection and transduction. However, we observed that over the low concentration range in our study, the aggregate sizes of n-TiO_2 + n-Ag mixtures varied between 300 nm and 500 nm (Fig. S11-b and -c), did not show an increase in size with an increase in concentration, and was unaffected by light or dark conditions. Thus, aggregation in the ENM mixtures is not a primary factor influencing phage infection when exposed to low concentrations of mixed n-TiO_2 and n-Ag under the conditions of this study. Additionally, the accumulation of a more toxic n-Ag/n-TiO_2 composite (Fig. 6f and S10) on host cells and phages may exert a combination of effects, such as inactivating phages by high ROS generation,[74] physically interfering with phage–cell interactions by blocking the recognition sites or phage entry at cell surface, and/or impairing phage-related membrane proteins as mentioned above, to disrupt phage entry into the cell.

ENM aggregation at the cell surface may also affect bacterial–phage electrostatic interactions.[22,33] In LMW (pH ∼ 8.3), the zeta potential of n-TiO_2 ranged from −14 to −15 mV under light or dark (Fig. S12). The zeta potential of n-Ag varies from −4 to −10 mV after 2 hours of exposure to light and the value becomes less negative as n-Ag concentration increases (Fig. S12-a). Under dark, n-Ag shows a more negative zeta potential, ranging from −9 to −12 mV (Fig. S12-b). Bacteria cells, like *E. coli*, are negatively charged in freshwater with an average zeta potential of −25 to −30 mV.[85] Phage particles are also negatively charged at neutral pH with zeta potential of around −39 mV.[86] Therefore, ENMs with less negative charge or patches of positive charge may reduce the repulsive electrostatic force between phages and cells, thereby contributing to favorable phage–cell interactions as indicated by the ENM effects on phage infection in Fig. 2. Although the zeta potential of n-TiO_2 + n-Ag mixtures is more negative than the two ENMs individually except for the mixtures containing 50 μg L^{-1} n-Ag under light (Fig. S12-a), the nanocomposite is still less negatively charged than either the bacteria or phage and can reduce repulsive interactions between phage and cell to a small degree. Thus, in contrast to previous reports, electrostatic interactions between the n-Ag/n-TiO_2 composite and cell or phage surfaces are unlikely to be more than a minor factor to explain the diminished phage infection of ENM mixtures under our experimental conditions.

3.4 Mechanistic effects of photoactive ENM exposure on phage entry and infection

We summarize the results of this study in Table S5 and illustrate possible mechanisms of interactions operating between ENMs, phage, and bacteria in Fig. 7.

Under light, pre-treatment with n-TiO_2 or n-Ag results in increased phage infections (Fig. 2a and c) through a number of potential interactions, among which the primary impact is increased OMP as detailed in our previous work.[41] A secondary interaction is related to potentially diminished negative charge on the phage capsid and/or bacterial surface due to exposure to individual ENMs, with n-Ag exerting a greater effect than n-TiO_2 (Fig. S12). *E. coli* exposure to photoactivated n-TiO_2 or n-Ag signals up-regulation of F-pili-related genes (with the effect on *traX* and *traV* greater than on *traA*) and increased pili density in patterns that follow the trends of phage infection results (Fig. 2, 4 and 6). Although ENM exposure under light or dark may trigger the expression of the *ompF* gene, the pattern of *ompF* gene expression does not follow the trends of OMP or phage infection measurements and thus, the OmpF protein is unlikely to be a key factor in promoting ENMs' influence on filamentous phage entry into the cell. Expression of the *tolAIII* gene is little affected by single ENM exposure under either light or dark conditions. While n-Ag has no effect on cell OMP under dark,[41] a slight increase in phage infection (Fig. 2d) is observed in samples pre-treated with n-Ag under dark,

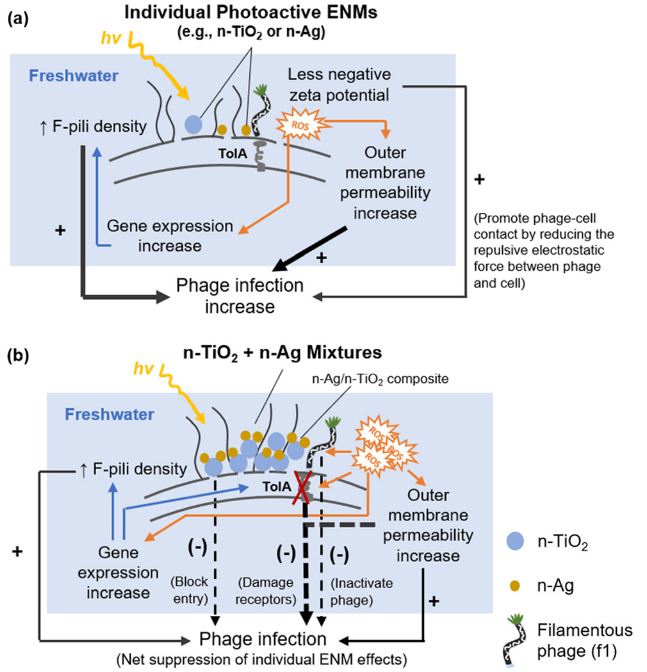

Fig. 7 Possible mechanisms of how (a) individual photoactive ENMs (*e.g.*, n-TiO$_2$ or n-Ag) and (b) the binary ENM mixtures under environmentally relevant conditions affect phage infection. Bold lines/arrows indicate significant contribution to ENMs' effects on phage infection, thin lines/arrows indicate minor contribution, "+" indicates a promoting effect, and "(-)" with dashed lines indicates a suppressing/inhibiting effect. The red "X" suggests possible damage by ROS.

possibly resulting from oxidative stress induced by released Ag$^+$ or favorable electrostatic interactions at the bacterial or phage surfaces due to Ag$^+$ sorption.[87] Overall, as illustrated in Fig. 7a, sublethal and environmentally relevant concentrations of n-TiO$_2$ or n-Ag under light generate ROS, damaging the outer membrane, increasing its permeability, triggering cellular stress, and stimulating gene expression that promotes F-pili formation and density. The combination of these effects enhances phage entry into the periplasmic space of the cell and results in increased phage infection.

In contrast to individual ENM exposure, phage infection in response to exposure to n-TiO$_2$ + n-Ag mixtures under light and the concomitant formation of n-Ag/n-TiO$_2$ composites show dissimilar trends with respect to OMP and select gene expression. When *E. coli* is pre-treated with n-TiO$_2$ + n-Ag mixtures, we observe an overall suppressing effect on phage infection compared to individual ENM effects under light or dark (Fig. 3), which at first glance seems inconsistent with the synergistic effects on increasing OMP,[41] gene expression (Fig. 5 and S6), or F-pili density (Fig. 6e) under light. Our previous work has detailed the formation of a self-assembled and highly reactive n-Ag/n-TiO$_2$ composite that produces higher ROS yields[42] and synergistically greater OMP[41] relative to individual ENM exposure, leading to damage to the periplasmic membrane protein TolA as evidenced by the up-regulation of the *tolAIII* gene (Fig. 5). Although F-pili-related genes are up-regulated and F-pili density increases, TolA damage disrupts the final steps of phage infection and explains why the greater OMP with exposure to the binary ENM mixtures results in suppressed rather than augmented phage infection, as illustrated in Fig. 7b. In addition, the ENM mixtures may also inactivate phage by increased ROS yields[74] and/or disrupt the phage–host interactions by attaching to phages or cells (Fig. 6f) and blocking receptors or entry for phage. The effects of n-Ag and dissolved Ag$^+$ on phage infection in the dark are also suppressed in the binary ENM mixtures (Fig. 3b) due to Ag$^+$ adsorption on the n-TiO$_2$ surface.[62]

4 Conclusion

In this study, we evaluate the impacts of n-TiO$_2$ and n-Ag at sublethal doses, individually and in mixtures, on the infection by filamentous phage f1 in a freshwater medium and interrogate how photoactive ENMs influence phage–bacterial interactions at a mechanistic level by exploring cell surface properties and the expression of select genes. Under light, n-TiO$_2$ or n-Ag induces measurable increases in phage infection, stimulates F-pili-related gene expression, and increases F-pili density in patterns consistent with increased OMP. Under dark, n-TiO$_2$ has minimal effect on phage infection, n-Ag induces slight increases, and neither of the two ENMs causes any significant changes to gene expression or F-pili formation. In contrast to individual ENM effects, exposure to binary ENM mixtures under light triggers large increases in OMP, F-pili-related gene expression, and pili density but suppresses phage infection, an effect likely related to damage to the membrane protein, TolA, which is critical to the phage infection process. These results detail the complex interactions between ENMs, phage, and cells to again demonstrate that synergistic interactions of ENM mixtures at sublethal concentrations under representative environmental conditions produce differential cellular responses in bacteria which are not predicted by effects of individual ENM exposure and are mediated by ROS-induced effects that increase OMP, modify cellular structures critical to phage entry to the host cell, and trigger cellular repair. Furthermore, these results suggest that sublethal, photoactive ENM stress may alter the mode and patterns of phage infection and future research is needed to explore such effects on microbial diversity and evolution over the long-term and the influence of other important environmental conditions, such as the quality and quantity of natural organic matter, hydrological factors, and the presence of other contaminants.

Author contributions

Shushan Wu: investigation, methodology, formal analysis, visualization, writing – original draft. Stefanie Huttelmaier: methodology, writing – review & editing. Jack Sumner: methodology, writing – review & editing. Erica Hartmann: writing – review & editing, resources. Kimberly Gray:

conceptualization, supervision, validation, writing – review & editing, resources.

Conflicts of interest

There are no conflicts to declare.

Data availability

Raw data (experiment results and measurements) and processed data used in this article are available at Dryad (DOI: https://doi.org/10.5061/dryad.1zcrjdg3r).

Supplementary information is available. See DOI: https://doi.org/10.1039/d5en00598a.

Acknowledgements

S/TEM imaging made use of the BioCryo facility (RRID: SCR_021288) of Northwestern University's NUANCE Center, which has received support from the SHyNE Resource (NSF ECCS-2025633), the IIN, and Northwestern's MRSEC program (NSF DMR-2308691). The Nano Zetasizer was from the Keck-II facility of Northwestern University's NUANCE Center, which has received support from the SHyNE Resource (NSF ECCS-2025633), the IIN, and Northwestern's MRSEC program (NSF DMR-1720139). Fig. 1 was created by https://Biorender.com. We are thankful to Nandini Budithi for her assistance in the phage infection experiment; Eric W. Roth for technical support with the S/TEM facility; Dr. McKenna Farmer for her help with laboratory techniques and basic experiment protocols; Dr. George Wells for his advice on experimental approach; and Dr. Yingqian Xiong for his assistance with the instrument operation and maintenance associated with the research. This research did not receive any specific grant from funding agencies in the public, commercial, or not-for-profit sectors.

References

1 T. Rambaran and R. Schirhagl, Nanotechnology from lab to industry - a look at current trends, *Nanoscale Adv.*, 2022, **4**(18), 3664–3675.

2 K. A. Bora, S. Hashmi, F. Zulfiqar, Z. Abideen, H. Ali, Z. S. Siddiqui and K. H. M. Siddique, Recent progress in bio-mediated synthesis and applications of engineered nanomaterials for sustainable agriculture, *Front. Plant Sci.*, 2022, **13**, 999505.

3 M. Roy, A. Roy, S. Rustagi and N. Pandey, An Overview of Nanomaterial Applications in Pharmacology, *BioMed Res. Int.*, 2023, **2023**, 4838043.

4 R. W. S. Lai, K. W. Y. Yeung, M. M. N. Yung, A. B. Djurisic, J. P. Giesy and K. M. Y. Leung, Regulation of engineered nanomaterials: current challenges, insights and future directions, *Environ. Sci. Pollut. Res.*, 2018, **25**(4), 3060–3077.

5 A. A. Keller, S. McFerran, A. Lazareva and S. Suh, Global life cycle releases of engineered nanomaterials, *J. Nanopart. Res.*, 2013, **15**(6), 1692.

6 A. Pietroiusti, H. Stockmann-Juvala, F. Lucaroni and K. Savolainen, Nanomaterial exposure, toxicity, and impact on human health, *Wiley Interdiscip. Rev.: Nanomed. Nanobiotechnol.*, 2018, **10**(5), e1513.

7 D. Surendhiran, H. Cui and L. Lin, Mode of Transfer, Toxicity and Negative Impacts of Engineered Nanoparticles on Environment, Human and Animal Health, in *The ELSI Handbook of Nanotechnology*, ed. C. M. Hussain, Scrivener Publishing LLC, 2020, pp. 165–204.

8 T. Tong, C. T. Binh, J. J. Kelly, J. F. Gaillard and K. A. Gray, Cytotoxicity of commercial nano-TiO2 to Escherichia coli assessed by high-throughput screening: effects of environmental factors, *Water Res.*, 2013, **47**(7), 2352–2362.

9 C. T. Binh, T. Tong, J. F. Gaillard, K. A. Gray and J. J. Kelly, Acute effects of TiO_2 nanomaterials on the viability and taxonomic composition of aquatic bacterial communities assessed via high-throughput screening and next generation sequencing, *PLoS One*, 2014, **9**(8), e106280.

10 Q. Abbas, B. Yousaf, H. Ullah, M. U. Ali, Y. S. Ok and J. Rinklebe, Environmental transformation and nano-toxicity of engineered nano-particles (ENPs) in aquatic and terrestrial organisms, *Crit. Rev. Environ. Sci. Technol.*, 2020, **50**(23), 2523–2581.

11 S. Wu, J. F. Gaillard and K. A. Gray, The impacts of metal-based engineered nanomaterial mixtures on microbial systems: A review, *Sci. Total Environ.*, 2021, **780**, 146496.

12 F. Rohwer, Global phage diversity, *Cell*, 2003, **113**(2), 141.

13 F. Torrella and R. Y. Morita, Evidence by Electron-Micrographs for a High-Incidence of Bacteriophage Particles in the Waters of Yaquina Bay, Oregon - Ecological and Taxonomical Implications, *Appl. Environ. Microbiol.*, 1979, **37**(4), 774–778.

14 O. Bergh, K. Y. Borsheim, G. Bratbak and M. Heldal, High Abundance of Viruses Found in Aquatic Environments, *Nature*, 1989, **340**(6233), 467–468.

15 S. Raza, M. Folga, M. Los, Z. Foltynowicz and J. Paczesny, The Effect of Zero-Valent Iron Nanoparticles (nZVI) on Bacteriophages, *Viruses*, 2022, **14**(5), 867.

16 R. Cheng, G. Q. Li, C. Cheng, P. Liu, L. Shi, Z. Ma and X. Zheng, Removal of bacteriophage f2 in water by nanoscale zero-valent iron and parameters optimization using response surface methodology, *Chem. Eng. J.*, 2014, **252**, 150–158.

17 R. Cheng, G. Q. Li, L. Shi, X. Y. Xue, M. Kang and X. Zheng, The mechanism for bacteriophage f2 removal by nanoscale zero-valent iron, *Water Res.*, 2016, **105**, 429–435.

18 R. Cheng, Y. Y. Zhang, T. Zhang, F. Hou, X. X. Cao, L. Shi, P. W. Jiang, X. Zheng and J. L. Wang, The inactivation of bacteriophages MS2 and PhiX174 by nanoscale zero-valent iron: Resistance difference and mechanisms, *Front. Environ. Sci. Eng.*, 2022, **16**(8), 108.

19 D. H. Yuan, L. X. Zhai, X. Y. Zhang, Y. Q. Cui, X. Y. Wang, Y. X. Zhao, H. D. Xu, L. S. He, C. L. Yan, R. Cheng, Y. Y. Kou and J. Q. Li, Study on the characteristics and mechanism of bacteriophage MS2 inactivated by bacterial cellulose supported nanoscale zero-valent iron, *J. Cleaner Prod.*, 2020, **270**, 122527.

20 E. Gilcrease, R. Williams and R. Goel, Evaluating the effect of silver nanoparticles on bacteriophage lytic infection cycle-a mechanistic understanding, *Water Res.*, 2020, **181**, 115900.

21 C. Cascio, O. Geiss, F. Franchini, I. Ojea-Jimenez, F. Rossi, D. Gilliland and L. Calzolai, Detection, quantification and derivation of number size distribution of silver nanoparticles in antimicrobial consumer products, *J. Anal. At. Spectrom.*, 2015, **30**(6), 1255–1265.

22 J. You, Y. Zhang and Z. Hu, Bacteria and bacteriophage inactivation by silver and zinc oxide nanoparticles, *Colloids Surf., B*, 2011, **85**, 161–167.

23 Q. Zhang, H. Zhou, P. Jiang, L. Wu and X. Xiao, Silver nanoparticles facilitate phage-borne resistance gene transfer in planktonic and microplastic-attached bacteria, *J. Hazard. Mater.*, 2024, **469**, 133942.

24 M. Colomer-Lluch, J. Jofre and M. Muniesa, Antibiotic resistance genes in the bacteriophage DNA fraction of environmental samples, *PLoS One*, 2011, **6**(3), e17549.

25 W. Calero-Caceres and M. Muniesa, Persistence of naturally occurring antibiotic resistance genes in the bacteria and bacteriophage fractions of wastewater, *Water Res.*, 2016, **95**, 11–18.

26 M. Muniesa, L. Imamovic and J. Jofre, Bacteriophages and genetic mobilization in sewage and faecally polluted environments, *Microb. Biotechnol.*, 2011, **4**(6), 725–734.

27 T. Kenzaka, K. Tani and M. Nasu, High-frequency phage-mediated gene transfer in freshwater environments determined at single-cell level, *ISME J.*, 2010, **4**(5), 648–659.

28 A. Y. Hassan, J. T. Lin, N. Ricker and H. Anany, The Age of Phage: Friend or Foe in the New Dawn of Therapeutic and Biocontrol Applications?, *Pharmaceuticals*, 2021, **14**(3), 199.

29 X. Han, P. Lv, L. G. Wang, F. Long, X. L. Ma, C. Liu, Y. J. Feng, M. F. Yang and X. Xiao, Impact of nano-TiO_2 on horizontal transfer of resistance genes mediated by filamentous phage transduction, *Environ. Sci.: Nano*, 2020, **7**(4), 1214–1224.

30 X. Xiao, X. L. Ma, X. Han, L. J. Wu, C. Liu and H. Q. Yu, TiO(2) photoexcitation promoted horizontal transfer of resistance genes mediated by phage transduction, *Sci. Total Environ.*, 2021, **760**, 144040.

31 J. H. Guo, S. H. Gao, J. Lu, P. L. Bond, W. Verstraete and Z. G. Yuan, Copper Oxide Nanoparticles Induce Lysogenic Bacteriophage and Metal-Resistance Genes in PAO1, *ACS Appl. Mater. Interfaces*, 2017, **9**(27), 22298–22307.

32 A. Nickel, M. Pedulla and R. Kasinath, The effect of nanoparticles on bacteriophage infections, in *NSTI-Nanotech 2010*, 2010, vol. 3.

33 X. Stachurska, K. Cendrowski, K. Pachnowska, A. Piegat, E. Mijowska and P. Nawrotek, Nanoparticles Influence Lytic Phage T4-like Performance In Vitro, *Int. J. Mol. Sci.*, 2022, **23**(13), 7179.

34 C. Howard-Varona, K. R. Hargreaves, S. T. Abedon and M. B. Sullivan, Lysogeny in nature: mechanisms, impact and ecology of temperate phages, *ISME J.*, 2017, **11**(7), 1511–1520.

35 M. G. Weinbauer, Ecology of prokaryotic viruses, *FEMS Microbiol. Rev.*, 2004, **28**(2), 127–181.

36 V. I. Syngouna and C. V. Chrysikopoulos, Inactivation of MS2 bacteriophage by titanium dioxide nanoparticles in the presence of quartz sand with and without ambient light, *J. Colloid Interface Sci.*, 2017, **497**, 117–125.

37 J. E. Lee and G. Ko, Norovirus and MS2 inactivation kinetics of UV-A and UV-B with and without TiO_2, *Water Res.*, 2013, **47**(15), 5607–5613.

38 Y. Koizumi and M. Taya, Kinetic evaluation of biocidal activity of titanium dioxide against phage MS2 considering interaction between the phage and photocatalyst particles, *Biochem. Eng. J.*, 2002, **12**(2), 107–116.

39 X. Zheng, Z. P. Shen, C. Cheng, L. Shi, R. Cheng and D. H. Yuan, Photocatalytic disinfection performance in virus and virus/bacteria system by Cu-TiO_2 nanofibers under visible light, *Environ. Pollut.*, 2018, **237**, 452–459.

40 J. Y. Kim, C. Lee, M. Cho and J. Yoon, Enhanced inactivation of E. coli and MS-2 phage by silver ions combined with UV-A and visible light irradiation, *Water Res.*, 2008, **42**(1–2), 356–362.

41 S. S. Wu, G. Wells and K. A. Gray, Engineered nanomaterials exert sublethal bacterial stress at very low doses: Effects of concentration, light, and media on cell membrane permeability, *Sci. Total Environ.*, 2024, **948**, 174861.

42 C. M. Wilke, B. Wunderlich, J. F. Gaillard and K. A. Gray, Synergistic Bacterial Stress Results from Exposure to Nano-Ag and Nano-TiO_2 Mixtures under Light in Environmental Media, *Environ. Sci. Technol.*, 2018, **52**(5), 3185–3194.

43 I. D. Hay and T. Lithgow, Filamentous phages: masters of a microbial sharing economy, *EMBO Rep.*, 2019, **20**(6), e47427.

44 S. Mantynen, E. Laanto, H. M. Oksanen, M. M. Poranen and S. L. Diaz-Munoz, Black box of phage-bacterium interactions: exploring alternative phage infection strategies, *Open Biol.*, 2021, **11**(9), 210188.

45 F. Karlsson, C. A. K. Borrebaeck, N. Nilsson and A. C. Malmborg-Hager, The mechanism of bacterial infection by filamentous phages involves molecular interactions between TolA and phage protein 3 domains, *J. Bacteriol.*, 2003, **185**(8), 2628–2634.

46 G. Guihard, P. Boulanger, H. Benedetti, R. Lloubes, M. Besnard and L. Letellier, Colicin A and the Tol Proteins Involved in Its Translocation Are Preferentially Located in the Contact Sites between the Inner and Outer Membranes of Escherichia Coli Cells, *J. Biol. Chem.*, 1994, **269**(8), 5874–5880.

47 L. Riechmann and P. Holliger, The C-terminal domain of ToIA is the coreceptor for filamentous phage infection of E. coli, *Cell*, 1997, **90**(2), 351–360.

48 Escherichia coli bacteriophage f1 - Handling Procedures, https://www.atcc.org/products/15766-b2.

49 R. A. Rodriguez, S. Bounty, S. Beck, C. Chan, C. McGuire and K. G. Linden, Photoreactivation of bacteriophages after UV disinfection: Role of genome structure and impacts of UV source, *Water Res.*, 2014, **55**, 143–149.

50 K. E. Wommack, R. T. Hill, T. A. Muller and R. R. Colwell, Effects of sunlight on bacteriophage viability and structure, *Appl. Environ. Microbiol.*, 1996, **62**(4), 1336–1341.

51 S. Guzman-Puyol, J. J. Benítez and J. A. Heredia-Guerrero, Transparency of polymeric food packaging materials, *Food Res. Int.*, 2022, **161**, 111792.

52 D. A. Russell and G. F. Hatfull, PhagesDB: the actinobacteriophage database, *Bioinformatics*, 2017, **33**(5), 784–786.

53 T. R. D. Costa, A. Ilangovan, M. Ukleja, A. Redzej, J. M. Santini, T. K. Smith, E. H. Egelman and G. Waksman, Structure of the Bacterial Sex F Pilus Reveals an Assembly of a Stoichiometric Protein-Phospholipid Complex, *Cell*, 2016, **166**(6), 1436–1444.e10.

54 D. McShan, P. C. Ray and H. T. Yu, Molecular toxicity mechanism of nanosilver, *J. Food Drug Anal.*, 2014, **22**(1), 116–127.

55 J. M. Hiller and A. Perlmutter, Effect of Zinc on Viral-Host Interactions in a Rainbow Trout Cell Line, Rtg-2, *Water Res.*, 1971, **5**(9), 703–710.

56 J. L. Speshock, R. C. Murdock, L. K. Braydich-Stolle, A. M. Schrand and S. M. Hussain, Interaction of silver nanoparticles with Tacaribe virus, *J. Nanobiotechnol.*, 2010, **8**, 19.

57 X. C. Jiang, C. Y. Chen, W. M. Chen and A. B. Yu, Role of Citric Acid in the Formation of Silver Nanoplates through a Synergistic Reduction Approach, *Langmuir*, 2010, **26**(6), 4400–4408.

58 L. Rudi, L. Cepoi, T. Chiriac, V. Miscu, A. Valuta and S. Djur, Effects of citrate-stabilized gold and silver nanoparticles on some safety parameters of Porphyridium cruentum biomass, *Front. Bioeng. Biotechnol.*, 2023, **11**, 1224945.

59 L. X. Chen, T. Rajh, Z. Y. Wang and M. C. Thurnauer, XAFS studies of surface structures of TiO2 nanoparticles and photocatalytic reduction of metal ions, *J. Phys. Chem. B*, 1997, **101**(50), 10688–10697.

60 K. E. Engates and H. J. Shipley, Adsorption of Pb, Cd, Cu, Zn, and Ni to titanium dioxide nanoparticles: effect of particle size, solid concentration, and exhaustion, *Environ. Sci. Pollut. Res.*, 2011, **18**(3), 386–395.

61 Q. R. Zhang, H. X. Zhou, J. Qiao, P. Jiang and X. Xiao, New insight into nanomaterial-mediated dissemination of phage-borne resistance genes: Roles of humic acid and illumination, *Chem. Eng. J.*, 2024, **486**, 150275.

62 C. M. Wilke, T. Tong, J. F. Gaillard and K. A. Gray, Attenuation of Microbial Stress Due to Nano-Ag and Nano-TiO_2 Interactions under Dark Conditions, *Environ. Sci. Technol.*, 2016, **50**, 11302–11310.

63 M. Mortimer, Y. Wang and P. A. Holden, Molecular Mechanisms of Nanomaterial-Bacterial Interactions Revealed by Omics-The Role of Nanomaterial Effect Level, *Front. Bioeng. Biotechnol.*, 2021, **9**, 683520.

64 M. Viveiros, M. Dupont, L. Rodrigues, I. Couto, A. Davin-Regli, M. Martins, J. M. Pages and L. Amaral, Antibiotic stress, genetic response and altered permeability of E. coli, *PLoS One*, 2007, **2**(4), e365.

65 D. Moore, C. M. Hamilton, K. Maneewannakul, Y. Mintz, L. S. Frost and K. Ippenihler, The Escherichia-Coli K-12 F-Plasmid Gene Trax Is Required for Acetylation of F-Pilin, *J. Bacteriol.*, 1993, **175**(5), 1375–1383.

66 R. L. Harris, V. Hombs and P. M. Silverman, Evidence that F-plasmid proteins TraV, TraK and TraB assemble. into an envelope-spanning structure in, *Mol. Microbiol.*, 2001, **42**(3), 757–766.

67 L. M. Stabryla, K. A. Johnston, J. E. Millstone and L. M. Gilbertson, Emerging investigator series: it's not all about the ion: support for particle-specific contributions to silver nanoparticle antimicrobial activity, *Environ. Sci.: Nano*, 2018, **5**(9), 2047–2068.

68 Y. C. Kim, A. W. Tarr and C. N. Penfold, Colicin import into cells: A model system for insights into the import mechanisms of bacteriocins, *Biochim. Biophys. Acta, Mol. Cell Res.*, 2014, **1843**(8), 1717–1731.

69 A. Sharma, S. P. Yadav, D. Sarma and A. Mukhopadhaya, Modulation of host cellular responses by gram-negative bacterial porins, *Adv. Protein Chem. Struct. Biol.*, 2022, **128**, 35–77.

70 R. Conners, R. I. León-Quezada, M. McLaren, N. J. Bennett, B. Daum, J. Rakonjac and V. A. M. Gold, Cryo-electron microscopy of the f1 filamentous phage reveals insights into viral infection and assembly, *Nat. Commun.*, 2023, **14**(1), 2724.

71 P. V. L. Reddy, B. Kavitha, P. A. K. Reddy and K. H. Kim, TiO_2-based photocatalytic disinfection of microbes in aqueous media: A review, *Environ. Res.*, 2017, **154**, 296–303.

72 O. Choi and Z. Hu, Size dependent and reactive oxygen species related nanosilver toxicity to nitrifying bacteria, *Environ. Sci. Technol.*, 2008, **42**(12), 4583–4588.

73 A. Onodera, F. Nishiumi, K. Kakiguchi, A. Tanaka, N. Tanabe, A. Honma, K. Yayama, Y. Yoshioka, K. Nakahira, S. Yonemura, I. Yanagihara, Y. Tsutsumi and Y. Kawai, Short-term changes in intracellular ROS localisation after the silver nanoparticles exposure depending on particle size, *Toxicol. Rep.*, 2015, **2**, 574–579.

74 G. Bastin, A. Galmiche, F. Talfournier, H. Mazon, J. Challant, M. Robin, D. Majou, N. Boudaud and C. Gantzer, Aerobic Conditions and Endogenous Reactive Oxygen Species Reduce the Production of Infectious MS2 Phage by Escherichia coli, *Viruses*, 2021, **13**(7), 1376.

75 K. C. Nikhil, S. Priyadarsini, M. Pashupathi, B. Ratta, M. Saxena, S. Ramakrishnan, P. Behera and A. Kumar, Regulatory Role of fnr Gene in Growth and tolA Gene Expression in Salmonella Typhimurium, *Indian J. Anim. Res.*, 2021, **55**(7), 774–779.

76 O. Metryka, D. Wasilkowski and A. Mrozik, Evaluation of the Effects of Ag, Cu, ZnO and TiO_2 Nanoparticles on the Expression Level of Oxidative Stress-Related Genes and the Activity of Antioxidant Enzymes in Escherichia coli, Bacillus cereus and Staphylococcus epidermidis, *Int. J. Mol. Sci.*, 2022, **23**(9), 4966.

77 H. G. Park and M. K. Yeo, Comparison of gene expression patterns from zebrafish embryos between pure silver

nanomaterial and mixed silver nanomaterial containing cells of, *Mol. Cell. Toxicol.*, 2015, **11**(3), 307–314.

78 M. Kulasza and L. Skuza, Changes of Gene Expression Patterns from Aquatic Organisms Exposed to Metal Nanoparticles, *Int. J. Environ. Res. Public Health*, 2021, **18**(16), 8361.

79 Y. Li, J. Yan, W. Ding, Y. Chen, L. M. Pack and T. Chen, Genotoxicity and gene expression analyses of liver and lung tissues of mice treated with titanium dioxide nanoparticles, *Mutagenesis*, 2017, **32**(1), 33–46.

80 C. L. Huang, I. L. Hsiao, H. C. Lin, C. F. Wang, Y. J. Huang and C. Y. Chuang, Silver nanoparticles affect on gene expression of inflammatory and neurodegenerative responses in mouse brain neural cells, *Environ. Res.*, 2015, **136**, 253–263.

81 X. D. Zhou and Y. Q. Li, *Atlas of oral microbiology: from healthy microflora to disease*, Elsevier/AP & Zhejiang University Press, 2015, p. 107.

82 C. C. Brinton, Jr., The structure, function, synthesis and genetic control of bacterial pili and a molecular model for DNA and RNA transport in gram negative bacteria, *Trans. N. Y. Acad. Sci.*, 1965, **27**(8), 1003–1054.

83 D. Zahrl, M. Wagner, K. Bischof and G. Koraimann, Expression and assembly of a functional type IV secretion system elicit extracytoplasmic and cytoplasmic stress responses in Escherichia coli, *J. Bacteriol.*, 2006, **188**(18), 6611–6621.

84 H. Bessaiah, C. Anamale, J. Sung and C. M. Dozois, What Flips the Switch? Signals and Stress Regulating Extraintestinal Pathogenic Escherichia coli Type 1 Fimbriae (Pili), *Microorganisms*, 2021, **10**(1), 5.

85 X. Liang, C. Y. Liao, M. L. Thompson, M. L. Soupir, L. R. Jarboe and P. M. Dixon, Surface Properties Differ between Stream Water and Sediment Environments, *Front. Microbiol.*, 2016, **7**, 1732.

86 A. Olszewska-Widdrat, M. Bennet, F. Mickoleit, M. Widdrat, C. Tarabout, V. Reichel, K. Arndt, D. Schüler and D. Faivre, Bacteriophage-Templated Assembly of Magnetic Nanoparticles and Their Actuation Potential, *Chem*, 2021, **7**(8), 942–949.

87 T. Ameh, M. Gibb, D. Stevens, S. H. Pradhan, E. Braswell and C. M. Sayes, Silver and Copper Nanoparticles Induce Oxidative Stress in Bacteria and Mammalian Cells, *Nanomaterials*, 2022, **12**(14), 2402.